



# **Tectonics**

# **RESEARCH ARTICLE**

10.1002/2016TC004400

#### **Key Points:**

- Detrital zircon geochronology constrains Maastrichtian through Oligocene sedimentation
- Changes in sediment provenance suggest Late Eocene uplift of the Frontal Cordillera
- Paleogene sedimentation rates track accelerating basin subsidence during Andean uplift

#### **Supporting Information:**

- · Supporting Information S1
- Figure S1
- Figure S2
- Table S1
- Table S2Table S3

#### **Correspondence to:**

J. C. Fosdick, julie.fosdick@uconn.edu

#### Citation:

Fosdick, J. C., E. J. Reat, B. Carrapa, G. Ortiz, and P. M. Alvarado (2017), Retroarc basin reorganization and aridification during Paleogene uplift of the southern central Andes, *Tectonics*, *36*, doi:10.1002/2016TC004400.

Received 20 OCT 2016 Accepted 22 FEB 2017 Accepted article online 23 FEB 2017

# Retroarc basin reorganization and aridification during Paleogene uplift of the southern central Andes

J. C. Fosdick<sup>1,2</sup>, E. J. Reat<sup>3</sup>, B. Carrapa<sup>4</sup>, G. Ortiz<sup>5</sup>, and P. M. Alvarado<sup>5</sup>

<sup>1</sup>Center for Integrative Geosciences, University of Connecticut, Storrs, Connecticut, USA, <sup>2</sup>Department of Geography, University of Connecticut, Storrs, Connecticut, USA, <sup>3</sup>Department of Geology and Geophysics, University of Utah, Salt Lake City, Utah, USA, <sup>4</sup>Department of Geosciences, University of Arizona, Tucson, Arizona, USA, <sup>5</sup>Centro de Investigaciones de la Geosfera y la Biosfera, Departamento de Geofísica y Astronomía, Facultad de Ciencias Exactas, Físicas y Naturales, Universidad Nacional de San Juan-Consejo Nacional de Investigaciones Científicas y Técnicas, San Juan, Argentina

**Abstract** Tectonic development of the Andean Cordillera has profoundly changed the topography, climate, and vegetation patterns of the southern central Andes. The Cenozoic Bermejo Basin in Argentina (~30°S) provides a key record of thrust belt kinematics and paleoclimate south of the high-elevation Puna Plateau. Ongoing debate regarding the timing of initiation of upper plate shortening and Andean uplift persists, precluding a thorough understanding of the earlier tectonic and climatic controls on basin evolution. We present new sedimentology, detrital geochronology, sandstone petrography, and subsidence analysis from the Bermejo Basin that reveal siliciclastic-evaporative fluvial and lacustrine environments prior to the main documented phase of Oligocene-Miocene shortening of the Frontal Cordillera and Argentine Precordillera. We report the first radiometric dates from detrital zircons collected in the Ciénaga del Río Huaco Formation, previously mapped as Permian, that constrain a Late Cretaceous (~95-93 Ma) maximum depositional age. Provenance and paleocurrent data from these strata indicate that detritus was derived from dissected arc and cratonic sources in the north and northeast. Detrital zircon U-Pb ages of ~37 Ma from the overlying red beds suggest that foredeep sedimentation began by at least the late Eocene. At this time, sediment dispersal shifted from axial southward to transversal eastward from the Andean Arc and Frontal Cordillera. Subsidence analysis of the basin fill is compatible with increasing tectonic deformation beginning in Eocene time, suggesting that a distal foredeep maintained fluvial connectivity to the hinterland during topographic uplift and unroofing of the Frontal Cordillera, prior to Oligocene-Miocene deformation across the Precordillera.

# 1. Introduction

Tectonics and climate through deformation, uplift, and erosion of the landscape shape the physiography of major orogenic belts and thereby control depositional environments and sediment dispersal. The modern Andean orogenic belt, which spans over 56° of latitude across several global atmospheric circulation cells (Figure 1a), exemplifies these interrelated processes. Along strike, the Andes exhibits highly variable topography, climate, deformational behavior, magmatism, slab and crustal seismicity, and distribution of retroarc foreland depocenters [e.g., Oncken et al., 2006; Alvarado et al., 2007; Strecker et al., 2007; Hilley and Coutand, 2010; Alvarado and Araujo, 2011; Pearson et al., 2012]. A central question in the Andes and elsewhere is to what extent aridification is driven solely by changes in global climate or development of an orographic barrier due to lithospheric shortening and surface uplift of upwind ranges. Feedbacks between precipitation, erosion, and tectonic stress, coupled with sparse temporal control on timing and rates, further impede our ability to evaluate this question. However, the sedimentary basin record of flexural subsidence may be the earliest archive of orogenic processes and growth and erosion of topography [Flemings and Jordan, 1990]. Accordingly, changes in sediment source areas, basin subsidence rate, and shifts in depositional environments reflect the local to regional tectonic and climatic framework superimposed by global climate [Willett, 1999; Barnes et al., 2012; Pingel et al., 2016].

In the southern central Andes, ongoing debate about the timing of initiation of upper plate shortening and uplift in the region persists. Understanding the early phase of retroarc foreland basin deformation is critical to better assess temporal estimates of shortening and the magnitude of underthrusting that may drive cycles in Cordilleran magmatism [DeCelles et al., 2009, 2015a], subduction slab inclination, and spatial shifts in major orogen-scale topographic divides. Much emphasis has been placed on the late Miocene uplift history of

©2017. American Geophysical Union. All Rights Reserved.

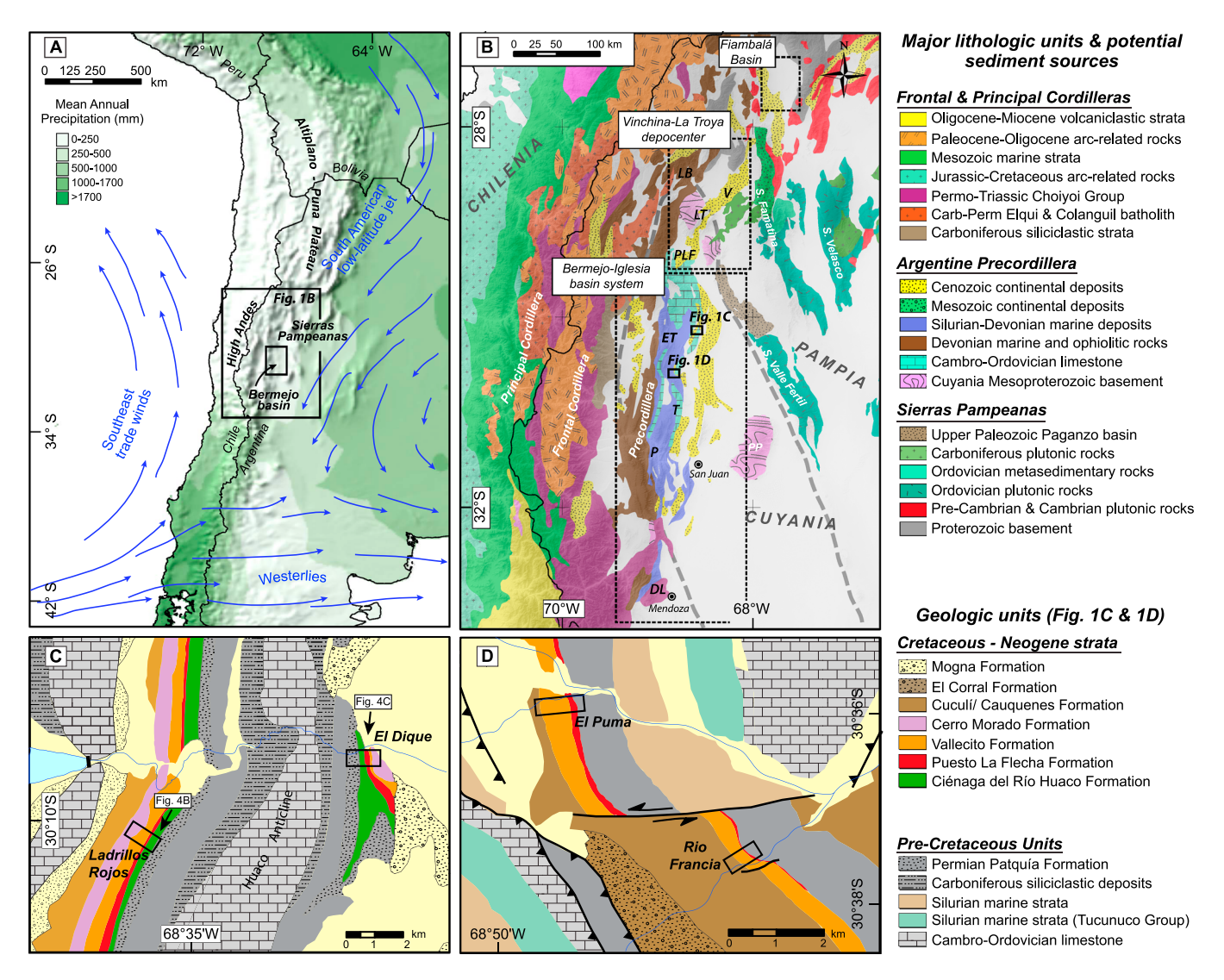


**Figure 1.** Geologic setting of the study area. (a) Precipitation and global circulation patterns in the central Andes. Blue arrows delineate vectors for mean 850 hPa winds for austral summer [Fiorella et al., 2015]. Mean annual precipitation data from Deichmann and Eklundh [1991]. (b) Regional geology and distribution of major source areas. Geology after Furque et al. [2003], SERNAGEOMIN [2003], Giambiagi et al. [2012], Ducea et al. [2015], Allmendinger and Judge [2014], and new mapping. Published stratigraphic studies referred to within the text include DL = Divisadero Largo [Yrigoyen, 1993; Folguera et al., 2001], LB = Laguna Brava [Vizán et al., 2013], LT = La Troya [Tedesco and Limarino, 2007; Ciccioli et al., 2011], P = Pachaco, T = Talacasto [Levina et al., 2014], and V = Vinchina [Limarino et al., 2001; Ciccioli et al., 2011, 2014]. Sections from this study: ET = El Templo, PLF = Puesto La Flecha, and RF = Río Francia. (c) Huaco Anticline study area showing locations of measured sections.

the central Andes [England and Molnar, 1990; Hoke and Garzione, 2008], while recent work in the central Andes has suggested a Paleocene onset of continuous foreland basin system development [Carrapa et al., 2008, 2012], eastward progression of surface uplift [Quade et al., 2015], and basin partitioning by Sierras Pampeanas intraforeland uplifts [Carrapa et al., 2008; Ciccioli et al., 2011; Carrapa and DeCelles, 2015; Safipour et al., 2015]. Although Paleogene foreland sedimentation is well documented in NW Argentina between 24 and 28°S [DeCelles et al., 2011; Carrapa et al., 2012], the early Cenozoic basin history between 28 and 34°S remains largely unconstrained and poorly documented, preventing a full understanding of what controls subduction margin segmentation, foreland basin connectivity, topographic evolution, and underlying geodynamic and surface processes.

This work sheds light on the Latest Cretaceous-Early Cenozoic (pre-22 Ma) Bermejo Basin in the southern central Andes, located south of the Altiplano-Puna Plateau and east of the Andean Cordillera (Figure 1), to evaluate how sedimentation styles, deformation patterns, and regional climate varied prior to the main

documented phase of Oligocene-Miocene construction of the Frontal Cordillera and Argentine Precordillera. Until recently, these pre-22 Ma deposits within the Bermejo Basin have been mapped as Permian-Triassic stratigraphy [Borello and Cuerda, 1968; Limarino et al., 2000] and therefore have been largely overlooked within the context of early Cenozoic climate and tectonic conditions. Previous stratigraphic and structural studies consider the onset of the foreland basin initiation and concomitant topographic growth of the Frontal Cordillera at ~22 Ma, based on the age of deposits interpreted as foredeep strata [Jordan et al., 2001; Levina et al., 2014].

This segment of the Andean orogen is important because it resides along a critical transitional position in the midlatitudes between hemispheric-scale atmospheric circulation patterns of the Easterlies and Westerlies, which influence regional climate zones and rainfall regimes (Figure 1a) [Garreaud et al., 2009]. North of ~30–31°S, the South American monsoon and South American low-level jet bring moisture to the Andean foreland from the east and northeast, and the orographic divide creates a major orographic barrier to the high-elevation Puna-Altiplano Plateau [Cook, 2003; Quade et al., 2015]. South of this latitudinal transition zone, the Westerlies carry moisture from the Pacific and Southern Oceans across the Andean Cordillera, generating an orographic rain shadow on the leeward side of the mountains (Figure 1a). However, the restored paleolatitude of the Bermejo Basin during mid-Cenozoic time may have been as far south as ~37°S (based on paleolatitude calculations following van Hinsbergen et al. [2015]), suggesting that northward movement of the South American plate caused this basin depocenter to pass from a leeward to windward position during basin history.

Here we address questions regarding the timing of sedimentation, source paleogeography, and tectonic setting of the basin strata. We further evaluate whether or not changes in depositional environment reflect predominantly aridification and cooling driven by global climate change [Zachos et al., 2008] or development of a local orographic barrier during Andean surface uplift [Canavan et al., 2014; Quade et al., 2015]. Answers to these questions have important implications for the growth history of Andean topography and climate conditions (i.e., moisture transfer and precipitation gradients) in a place where major atmospheric circulation cells converge. New sedimentology and geochronology of detrital zircons and interbedded volcanic ash from strata previously considered to be preforeland basin provide provenance and chronology constraints to quantify sedimentation rate and style during Late Cretaceous and Oligocene time. Our findings require a reevaluation of the paleogeography and tectonic history during this important interval. We confirm and refine the timing of Cretaceous sedimentation and present new evidence of Late Cretaceous alluvial deposits derived from the northeast and affected by inherited paleogeography in a retroarc foreland basin setting. We also report the first Eocene strata within the Bermejo Basin that preserve a climatic shift from fluvial-lacustrine environments with gypsum, indicating semiarid conditions, to the culmination of major eolian dune fields at the Eocene-Oligocene transition. Taken together along the Andean orogen, these are the oldest recognized Cenozoic eolian deposits during this phase of foreland basin evolution.

# 2. Geologic Background

# 2.1. Basin Geodynamics

The Bermejo Basin is a retroarc foreland basin situated ~30–33°S above the Chilean-Pampean flat slab segment in the southern central Andes (Figure 1). It is structurally bound to the west by the Argentine Precordillera fold-and-thrust belt and intervening wedge-top basins and the high-elevation Frontal and Principal Cordilleras [Ramos et al., 1996; Ammirati et al., 2016]. To the east, the Bermejo Basin is bound by the Sierras Pampeanas fault-bounded basement-cored uplifts, namely, the Sierra de Valle Fértil and Sierra de Pie de Palo (Figure 1b). The basin contains >4 km thick sedimentary infill of mostly Oligocene-Miocene strata [Johnson et al., 1986; Jordan et al., 1993, 2001] and has been classically studied as an example of retroarc foreland basin. Its older strata are structurally deformed by the eastern Argentine Precordillera [Zapata, 1998]. The Bermejo Basin developed atop the Cuyania microplate, an allochthonous terrane that was accreted to Gondwana during Paleozoic time [Thomas and Astini, 1996; Ramos, 2004]. Pre-Cenozoic tectonic and deformational events have affected the retroarc lithosphere in northwest Argentina [Ramos and Aleman, 2000; Charrier et al., 2014], including Carboniferous-Permian transtensional extension and formation of the Paganzo Basin depocenter (Figure 1b). Continued Mesozoic intracontinental rifting resulted in the development of Triassic Cuyo and Ischigualasto rifts [Fernandez-Seveso et al., 1995; Tankard et al., 1995] that

	Bermejo basin (Huaco)										Vinchina-La Troya basins		
	Bracaccini 1946	Furque 1979		Limarino et al. 1987		'érez et al. 1993	Jordan et al. 1993	Limarino et al. 2000	This study	Ciccioli et al. 2014			
Tri	assic (?) eolian sandstone	Vallecito Fm. (Triassic)		Vallecito Member	Cretaceous	eolian sandstone	Vallecito Fm. (Oligocene)	Vallecito Fm. (Neogene)	Vallecito Fm. (Oligocene) ~33-23 <b>M</b> a		Vallecito Fm. Late Oligocene - early Miocene)		
Paganzo (Permian?)	Red sandstone, claystone, and siltstone complex	Ojo de Agua (Permian)		Ojo de Agua Member		basal unit	Permian red beds	Red beds (Tertiary)	Paleocene - Eocene (~65-36 Ma)  Ciénaga del Río Huaco Fm. (Upper Cretaceous)		Puesto La Flecha Fm (Late Eocene -		
								Ciénaga del Río Huaco Fm. (Upper Cretaceous)			Oligocene) Ciénaga del		
						Patquía Fm.		(Opper Cretaceous)	ca. 96-93 Ma		Río Huaco Fm. (Upper Cretaceous)		
						(Permian)		Patquía Fm. (Permian)	Patquía Fm. (Permian)		Late Paleozoic Fms.		

**Figure 2.** Summary of previous stratigraphic subdivisions of the Bermejo Basin in the Huaco Anticline area and the stratigraphic nomenclature used in this study (strata overlying the Vallecito Formation are not included; see text for discussion). The generalized stratigraphy of the Vinchina-La Troya depocenter, located north of the Bermejo Basin, is shown for comparison [*Ciccioli et al.*, 2014].

partitioned the Cuyania and Pampean basement. Changes in subduction mode along the South American margin caused a shift from back arc and intraarc extension between 150 and 115 Ma during which time, northwest trending transtensional depocenters formed east of the Bermejo Basin [*Tankard et al.*, 1995]. By ~115 Ma, a compressive retroarc regime led to upper plate shortening [*Ramos and Aleman*, 2000].

In the retroarc foreland region, well-documented Oligocene foredeep sedimentation began at ~22 Ma [Jordan et al., 1993, 2001], and a close progression of Miocene-Pliocene deformation and exhumation across the Argentine Precordillera have been described [Allmendinger et al., 1990; Zapata and Allmendinger, 1996; Suriano et al., 2011; Allmendinger and Judge, 2014; Fosdick et al., 2015; Val et al., 2016]. Coeval inversion of intraarc basins in Oligocene time indicates localized extension within the arc [Godoy et al., 1999], leading many to argue against contraction within the retroarc foreland area prior to Miocene basin inversion. Beginning at ~10–6 Ma, the subduction angle shallowed [Kay et al., 1991], leading to the modern flat slab conditions beneath the Sierras Pampeanas [Ramos et al., 2002; Ammirati et al., 2016] and disruption of the foreland basin.

Recent studies farther north in the Vinchina Basin and La Troya Basins (Figure 1), together with existing data for the Bermejo Basin, have led to several important revisions to the Late Mesozoic and Cenozoic stratigraphy in northwestern Argentina: (1) presence of Cretaceous strata, (2) an Oligocene-Miocene age for the Vallecito Formation, and (3) preservation of Cenozoic hematite-bearing siliciclastics (e.g., red beds) underlying the Vallecito Formation [Ciccioli et al., 2005, 2011, 2014; Tedesco and Limarino, 2007; Ariza, 2009] (Figure 2). The recently discovered dinosaur fossils [Tello, 2013] and microfossils [Limarino et al., 2000] within the red beds in the Ciénaga Preserve support an important age revision and recognition of a Cretaceous unit—the Ciénaga del Río Huaco Formation—which overlies the Permian Patquía Formation Upper Cretaceous and Paleogene strata are also present in the Cuyo Basin south of the study area near Mendoza (Figure 1) [Yrigoyen, 1993; Irigoyen et al., 2000], although the detailed chronology and lateral correlation of these strata with units in our study area are unclear. In the study area, a regional eolian-dominated unit, the Vallecito Formation rests on top of the Ciénaga del Río Huaco Formation [Jordan et al., 1993; Milana et al., 2003; Tripaldi and Limarino, 2005; Soria, 2010].

### 2.2. Climatic Conditions

The Argentina Precordillera resides in a semiarid setting at an average elevation of 700 m (basin) to 3000 m (range peaks) with less than 250 mm yr<sup>-1</sup> mean annual rainfall [Bookhagen and Strecker, 2012]. Our study area is today within this transition zone and receives mixed precipitation from both westerly and easterly sources but is generally dry. This global wind transition zone occurs at ~32°S, with variation in position between 28 and 35°S depending on seasonal and long-term climate variations. The largest precipitation gradient occurs between 30 and 35°S (Figure 1). Distributed topography of the Sierras Pampeanas generates weak gradients in rainfall and local orographic barriers to eastern moisture (Figure 1a). Evaporites can be used as a proxy for



arid climatic conditions. In general, the age of the oldest evaporite deposits decreases eastward [Quade et al., 2015], so our locality preserves some of the older remnants of hydrologically closed basins.

#### 2.3. Basin Stratigraphy

Here we briefly describe the general basin stratigraphy and unit designation in order to provide context for the new constraints on depositional age. The Bermejo Basin contains mostly Mesozoic and Cenozoic siliciclastic nonmarine sandstone, siltstone, mudstone, and conglomerate. Owing to their similar facies, the continental red beds in the Huaco Anticline were initially grouped together and mapped as the Permian Paganzo Formation [Bracaccini, 1946]. Subsequent studies have further subdivided these strata into the Ojo de Agua Member and overlying eolian Vallecito Member and the Patguía Formation [Limarino et al., 1987; Milana, 1993]. In the Huaco Anticline area, Limarino et al. [2000] more recently reclassified the upper part of the Patquía Formation as Upper Cretaceous fluvial and lacustrine strata, formally called the Ciénaga del Río Huaco Formation (CRH), based on Maastrichtian ostracod and palynomorph fossils. In its type locality Limarino et al. [2000] defined the CRH as a lower conglomeratic member, middle meandering stream member, and upper lacustrine facies. The coarse-grained basal CRH, rich in rounded quartz and fine-grained igneous clasts, forms an erosional disconformity into the underlying Patquía Formation [Limarino et al., 2000; Soria, 2010]. Dinosaur footprints have been found within these strata, further supporting a Cretaceous age [Tello, 2013]. The CRH has been recognized farther north in the Vinchina area (Figure 1), where Ciccioli et al. [2005] reported Maastrichtian microfossils and interpreted the unit as representative of an arid to semiarid lacustrine system. In the La Troya river area (La Rioja Province), a K-Ar age of 108 ± 4.4 Ma was obtained from interbedded volcanic ash [Tedesco and Limarino, 2007]. However, no radiometric data are reported from the CRH in the Bermejo Basin.

Above the CRH in the Bermejo Basin, Limarino et al. [2000] describe "Tertiary red beds" overlain by the eolian Vallecito Formation in the Río Huaco Group [Borello and Cuerda, 1968]. However, few studies exist on the sedimentology and basin subsidence history of the intervening red beds succession that crop out discontinuously beneath the Vallecito Formation [Limarino et al., 1987; Ariza, 2009; Soria, 2010]. Farther north in the Vinchina and La Troya areas, this red bed stratigraphic interval beneath the Vallecito Formation is called the Puesto La Flecha Formation [Caselli, 2002; Ciccioli et al., 2014]. De La Fuente et al. [2003] suggested an Oligocene age for these deposits, but a Paleocene-early Eocene age has also been proposed [Krapovickas et al., 2009]. The Puesto La Flecha Formation, in its type locality, is composed of fine-grained sandstone and shale deposited in ephemeral sandy stream and shallow lacustrine systems. Caselli [2002] was first to note a correlation of the red beds in the El Fiscal area of the Bermejo Basin to the Puesto La Flecha Formation in the La Rioja Province. Following the nomenclature of Ciccioli et al. [2014] and based on sedimentological similarities, we suggest that these deposits are indeed correlative to the Puesto La Flecha Formation and hereafter we refer to this distinctive red bed series as such in the Bermejo Basin (Figure 2). Also in the north, the Laguna Brava Formation yields an Eocene age based on paleomagnetic study [Vizán et al., 2013], which represents a lateral continuation of the Puesto La Flecha Formation In this study, we focus on the timing of sedimentation and paleogeography of the earlier basin history of the Bermejo Basin.

Jordan et al. [1993] and Peréz et al. [1993] report Oligocene zircon fission track ages from these eolian strata, which have since been interpreted as the base of the synorogenic foreland basin phase that includes the Miocene fluvial and alluvial facies of the Bermejo Basin [Jordan et al., 2001]. Younger Miocene-Pliocene alluvial strata overlie the Vallecito Formation and locally have different names across the study area reflecting local depositional environment and provenance. In the Huaco Anticline area, Vallecito Formation ranges in thickness from 70 to 350 m and is disconformably overlain by the volcaniclastic Cerro Morado Formation, a matrix-supported andesitic breccia with local intercalations of rippled brick red mudstone and siltstone. Clast compositions are mostly andesite, with trachytic andesite, and basaltic andesite. The Cerro Morado Formation is locally restricted and has an erosive basal unconformity, thereby cutting down into underlying strata. The Cerro Morado Formation consists of andesitic volcanic flows, pyroclastic flows, volcaniclastic breccias, and alluvial fans, with a source area in the northern Precordillera [Limarino et al., 2002]. Zircon fission track data from andesite clasts suggest an eruptive age of ~13.4 Ma [Jordan et al., 1993], though the full duration of the Cerro Morado is debated [Limarino et al., 2002]. Above the middle Miocene Cerro Morado Formation, the late Miocene Los Cauquenes Formation consists of sandstone and conglomerate [Limarino et al., 1987; Furque et al., 2003]. Near Huaco, the Jarillal Formation through Río Jáchal Formations consists

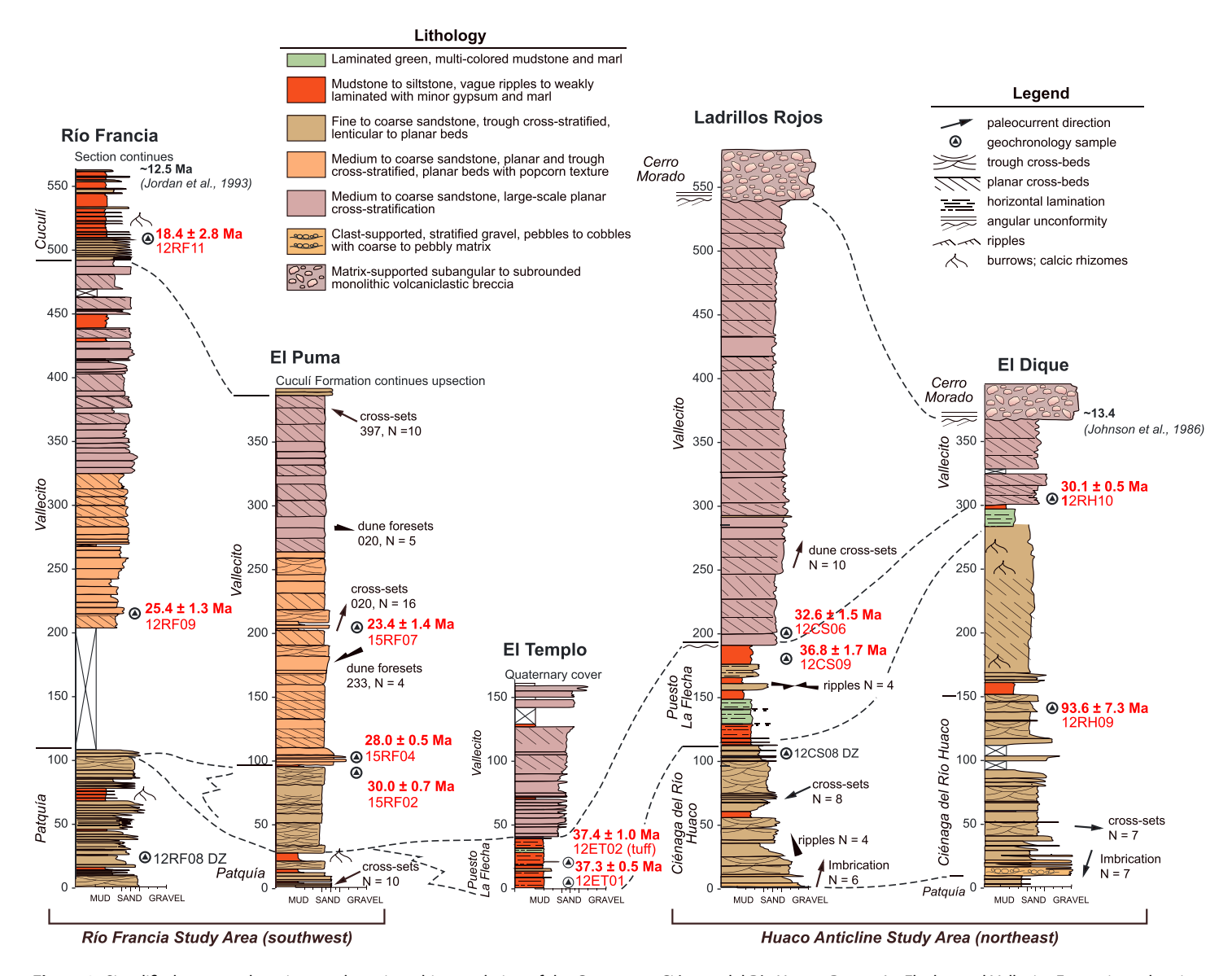


**Figure 3.** Simplified measured sections and stratigraphic correlation of the Cretaceous Ciénaga del Río Huaco, Puesto La Flecha, and Vallecito Formations showing summary of geochronology sample positions (maximum depositional ages in red text) and changes in depositional style across the study area. Refer to Figure 1 for locations of sections.

of a continuous sedimentary record from 16 to 4 Ma [Johnson et al., 1986; Jordan et al., 1993; Milana et al., 2003]. Near Río Francia (Río Azul) the basin record is ~22 to 9 Ma old [Jordan et al., 1990] and includes the Cuculí Formation and the conglomeratic El Corral Formation [Furque et al., 2003].

# 3. Methods and Results

# 3.1. Sedimentology

We conducted field mapping and sedimentary facies analysis of a ~2040 m thick composite measured stratigraphic section from five localities in the Bermejo Basin, focusing on the Ciénaga del Río Huaco, overlying Puesto La Flecha, and Vallecito Formations (Figure 3). Lithological descriptions, bed thicknesses, facies, and sedimentary structures were described at decimeter scale. Where preserved, paleoflow directions were determined from the orientations of ripples, imbricated conglomerate clasts, and the limbs of trough cross stratification. Samples were collected for thin section sandstone petrography and detrital zircon geochronology. Lithofacies shown in Table 1 are modified from *Miall* [1978] and *DeCelles et al.* [2015b].



Lithofacies Code	Description	Interpretation
Gmm	Massive, matrix-supported pebble to boulder conglomerate, poorly sorted, unstratified, silty sandstone matrix	Deposition in semicohesive matrix-supported debris flows and hyperconcentrated flows
Gct	Matrix-supported pebble to cobble conglomerate, moderately sorted, trough cross stratification	Channel fill deposits
Gch	Clast-supported pebble to cobble conglomerate, well sorted, horizontally stratified, imbricated	Deposition from shallow traction currents in longitudinal bars and gravel sheets
Sm	Massive medium- to fine-grained sandstones; bioturbated	Bioturbated sand; overbank deposits
Sr	Fine-grained to very fine grained sandstone with asymmetric current ripples	Migration of small ripples under weak unidirectional flows in shallow channels
Srw	Fine-grained to very fine grained sandstone with symmetrical ripples	Deposition in oscillatory current ripples in shallow lakes and ponds
St	Medium- to coarse-grained sandstones with trough cross stratification	Migration of subaqueous dunes under moderately powerful unidirectional flows in large channels
Spt	Fine- to coarse-grained sandstone with planar or tangential cross-stratification, popcorn weathering texture	Interdune (fluvial-eolian) deposits
Sp	Fine- to coarse-grained sandstone with large-scale (>2 m) planar cross stratification	Migration of eolian dunes
Sh	Fine- to coarse-grained sandstone with planar cross stratification	Upper plane bed conditions under unidirectional flow
FsI	Laminated mudstone and siltstone	Suspension settling in ponds and lakes
Fr	Mudstone and siltstone, ripple laminations	Suspension settling in ponds, lakes, and overbanks
C	Coal, carbonaceous mud	Swamp deposits
Eg	Evaporite gypsum	Dry playa surface



**Figure 4.** Panoramic photographs of the stratigraphy exposed in the Huaco Anticline. (a) View looking northeast through the upper sandstone beds of the Ciénaga del Rio Huaco Formation and overlying eolian Vallecito Formation and overlying, cliff-forming Cerro Morado Formation. (b) View of the Ladrillos Rojos section looking along strike to the south.

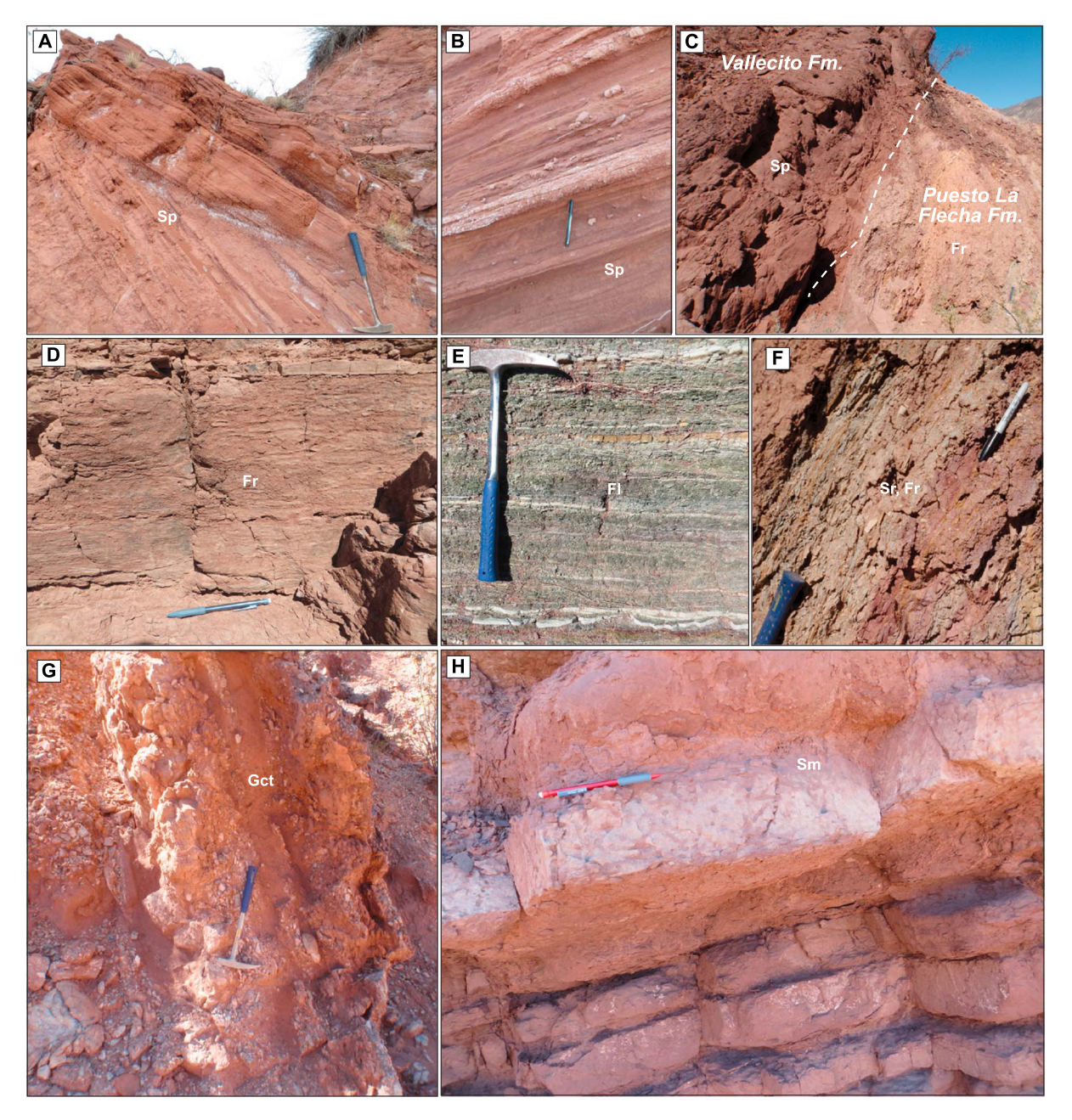


**Figure 5.** Selected outcrop photographs of the Ciénaga del Río Huaco, Puesto La Flecha, and Vallecito Formations in the Bermejo Basin. (a) Large-scale dune cross-stratified sandstone; (b) close-up of grain flow laminations within *Sp* and popcorn weathering texture; (c) contact between eolian Vallecito Formation and underlying rippled siltstone-mudstone, *Fr*, of the Puesto La Flecha Formation; (d) rippled fine-grained sandstone, *Sr*, the Puesto La Flecha Formation; (e) thinly bedded green, purple, and yellowish siltstone and mudstone, *Fsl* and *Fr*, the Puesto La Flecha Formation; (f) rippled green, purple, and yellowish siltstone; (g) matrix-supported, cross-stratified conglomerate and sandstone, *Gct* and *St*, Ciénaga del Río Huaco Formation; and (h) heavily bioturbated, channelized sandstone, *Sm*, Ciénaga del Río Huaco Formation.

# 3.1.1. Ciénaga del Río Huaco (Upper Cretaceous-Paleocene)

In the type locality of the Huaco Anticline area, the Ciénaga del Río Huaco Formation (CRH) is well exposed and rests disconformably on the Permian Patquía Formation (Figure 4). This basal unconformity exhibits up to 70 m of erosional relief into the underlying Patquía Formation. Lateral continuity of the outcrop belt preserves ~25 km of continuous fluvial deposits. Across the study area the CRH ranges in thickness from ~100 to 150 m and consists of reddish brown trough cross-stratified pebble to cobble conglomerate beds (*Gct*) that fine upward into trough cross-bedded sandstone (*St*) and rippled siltstone (*Sr*) (Figures 5g and 5h). Beds exhibit broad lenticular geometry and erosional basal surfaces. Lateral variations in the magnitude

of bioturbation (Figure 5h; tubular calcified rhizoliths and burrows) and pedogenesis indicate subaerial wetting and drying of an overbank environment. The CRH thins laterally to the southwest and is not exposed in the Río Francia area. Conglomerates are composed of predominantly well-rounded, polished quartzite and aphanitic volcanic clasts supported by a muddy siltstone matrix. Paleocurrent measurements indicate a predominantly S-SW paleoflow in the basal conglomerate, with upsection shift to W-SW directed paleoflow in the channelized trough cross-bedded strata (Figure 3).

# 3.1.2. Puesto La Flecha Formation (Paleocene to ~36 Ma)

The Puesto La Flecha Formation is exposed in the Huaco Anticline and El Templo areas and thins laterally to the south (Figures 1 and 3). In the Ladrillos Rojos section, the underlying conglomeratic CRH grades upward into thinly bedded mudstone of the Puesto La Flecha Formation (Figure 3). Here we differentiate the Puesto La Flecha Formation from the underlying fluvial CRH strata based on its recessive outcrops of horizontally laminated and rippled green, gray, maroon, and yellow siltstone (*Fsl*), with interbedded thick (>1 m) gypsum beds (*Em*) and fine-grained sandstone (*Fsl*, *Fr*). The gypsum deposits are laterally extensive and discontinuous, with thickest exposure in Ladrillos Rojos section (Figure 4). The Puesto La Flecha Formation is ~40 m thick and consists of poorly lithified orange to brick red rippled siltstone and interbedded massive fine-grained sandstone (*Sr*, *Sm*, *Fsl*, *Fr*, and *C*). The Puesto La Flecha Formation is well exposed in the Huaco Anticline and El Templo areas and thins laterally to the south (Figure 3). Where preserved and measurable, asymmetric ripple orientations indicate eastward directed paleoflow (Figure 3).

#### 3.1.3. Vallecito Formation (Lower Oligocene-Lower Miocene, ~30 to 23 Ma)

The Vallecito Formation consists of maroon, gray, and brightly orange colored large-scale planar cross-bedded sandstone (*Sp, Spt*). Bed set thickness ranges from 1 to 8 m, with 2–3 cm scale grain flow lamination in medium- to coarse-grained sandstones (Figure 5b). In all localities the Vallecito Formation transitions in color upsection from reddish orange to greenish tan. Bright orange beds in the lower unit exhibit large-scale tangential cross stratification (*Spt*), pitted and frosted quartz grains, and popcorn texture, which is especially well developed in the El Puma section (Figures 5a and 5b). Upsection, this formation is more strongly lithified and cemented and shows a uniform maroon color. Paleocurrent data suggest paleowind direction from the west to southwest, based on the orientation of planar cross stratification.

# 3.2. Provenance of Sandstone and Detrital Zircons

### 3.2.1. Sandstone Petrography

Eleven samples from medium- to fine-grained sandstones were collected from the Ciénaga del Río Huaco, Puesto La Flecha, and Vallecito Formations for petrographic analysis and detrital zircon geochronology. For a provenance comparison, we also point counted samples from the underlying Permian Patquía Formation and overlying Miocene Jarillal Formation (Figure 6). Each thin section was stained for potassium feldspar, and 400 framework grains were counted following the Gazzi-Dickinson method [Ingersoll et al., 1984; Dickinson, 1985]. Grain parameters identified in these point counts are listed in the data repository, and recalculated data are provided in Table 2.

In thin section, CRH sandstones are well sorted, with framework grains surrounded by a fine silt matrix and calcite cement. Dominant grain types include monocrystalline and polycrystalline quartz, plagioclase, potassium feldspar, and a variety of metamorphic lithic fragments of mostly schist and gneiss. Rare intermediate lathwork volcanic grains are present. Accessory minerals include magnetite, white mica, biotite, pyroxene, iron oxides, and zircon. The CRH sandstones are moderately lithified feldspathic litharenites with <5% mud matrix and plot within the recycled orogen (Qm-F-Lt) and craton interior (Qt-F-L) fields of Dickinson [1985] (Figure 6).

In thin section, sandstones from the Puesto La Flecha Formation are dominated by monocrystalline and polycrystalline quartz, plagioclase, potassium feldspar, and abundant lithic fragments. Lithic grain compositions are mostly intermediate volcanics with lathwork texture, gneiss, schist, with lesser amounts of siltstone, and shale. Accessory minerals include magnetite, amphibole, biotite, pyroxene, white mica, and epidote. The Puesto La Flecha (PLF) sandstones are lithic arkose to feldspathic litharenites with quartz and calcite cement and plot within the transitional (*Qm-F-Lt*) to dissected arc (*Qt-F-L*) fields. Only one sample from the basal PLF with high *Qm* and *Lm* plots within recycled orogen and deeply dissected arc.

Sandstones from the Vallecito Formation are dominated by monocrystalline quartz, plagioclase, potassium feldspar, polycrystalline, and abundant lithic fragments. In thin section, the Vallecito Formation consists of

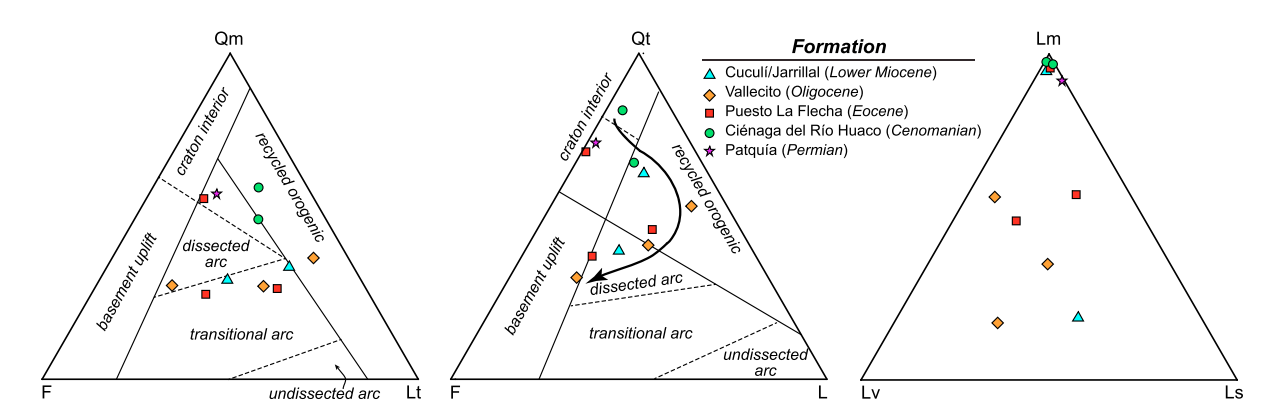


**Figure 6.** Sandstone modal petrographic data from the Ciénaga del Río Huaco, Puesto La Flecha, and Vallecito Formations. Samples from the bounding Permian Patquía and Miocene Cuculí and Jarillal Formations are included for comparison. Refer to Table 2 for parameters. Tectonic provenance fields are from *Dickinson* [1985].

lithic arenite with grain-supported subrounded to well-rounded grains, with <5% matrix and a calcite and iron oxide cement. Lithic grain compositions are mostly intermediate volcanics, and sedimentary lithics including siltstone, with lesser amounts of shale. Metamorphic lithic grains are rare. Accessory minerals include pyroxene, amphibole, magnetite, and biotite. Sandstones of the Vallecito Formation range in compositions from arkose to litharenites and plot within the dissected to transitional arc fields of *Dickinson* [1985]. Only one sample from the Vallecito Formation near Río Francia with high *Qm* and *Lm* plots within recycled orogen.

# 3.2.2. Detrital Zircon U-Pb Geochronology

Zircon extractions from 14 sandstones and 1 volcanic ash sample were carried out using standard crushing and sizing procedures following the methods in *Gehrels et al.* [2006]. Final zircon concentrates were inspected under a binocular microscope to remove obvious contaminants, mounted on tape in epoxy resin, and only polished to expose the interior of the grain. U-Pb detrital zircon geochronology was conducted by laser ablation inductively coupled plasma mass spectrometry at the LaserChron Center at the University of Arizona. Detrital zircons were randomly analyzed from a linear swath of grains across the sample mount to minimize sampling bias in characterizing all detrital populations. Full analytical results and data reduction methods are reported in the supporting information. Detrital zircon U-Pb results are displayed as linear age plots with corresponding relative probability distributions in ascending stratigraphic order (Figure 7). For samples that yielded the youngest age groups that could represent conceivable depositional ages, we calculated maximum depositional ages (MDA) using the following criteria: error-weighted mean ages for populations of concordant grains ( $^{206}$ Pb/ $^{238}$ U and  $^{207}$ Pb/ $^{235}$ U ages within 10% concordance) and overlapping ages at  $^{20}$  uncertainty.

# 3.2.2.1. Ciénaga del Río Huaco Formation

Sample 12RH09 yielded zircon U-Pb ages between 93 and 2720 Ma (n = 122 grains). Dominant age groups are 275–330 Ma, 510–775 Ma, 835–1510 Ma, and a smaller age cluster between 400 and 505 Ma (Figure 7). MDA

	Qm	F	Lt	Qt	F	L	Qm	Р	K	Lm	Lv	Ls
Sample	(%)	(%)	(%)	(%)	(%)	(%)	(%)	(%)	(%)	(%)	(%)	(%)
12CS08	28	23	49	46	23	31	55	26	19	57	14	29
12ET01	55	29	15	70	29	1	76	16	8	95	2	2
12HC02	34	17	49	63	17	20	68	12	20	95	3	2
12JT12	26	43	30	38	43	19	49	24	27	49	34	17
12RF08	57	25	18	73	25	2	69	22	9	92	0	8
12RF09	37	9	53	53	9	38	82	15	3	56	36	7
12RF10	30	35	34	39	35	25	46	30	24	19	33	48
12RH10	28	27	45	41	27	32	54	21	25	36	33	32
12RHS01	59	13	28	83	13	4	83	11	7	97	0	3
12RHS03	29	51	20	31	51	18	36	42	22	18	55	27
15CS01	49	18	33	67	18	15	74	15	10	98	2	0

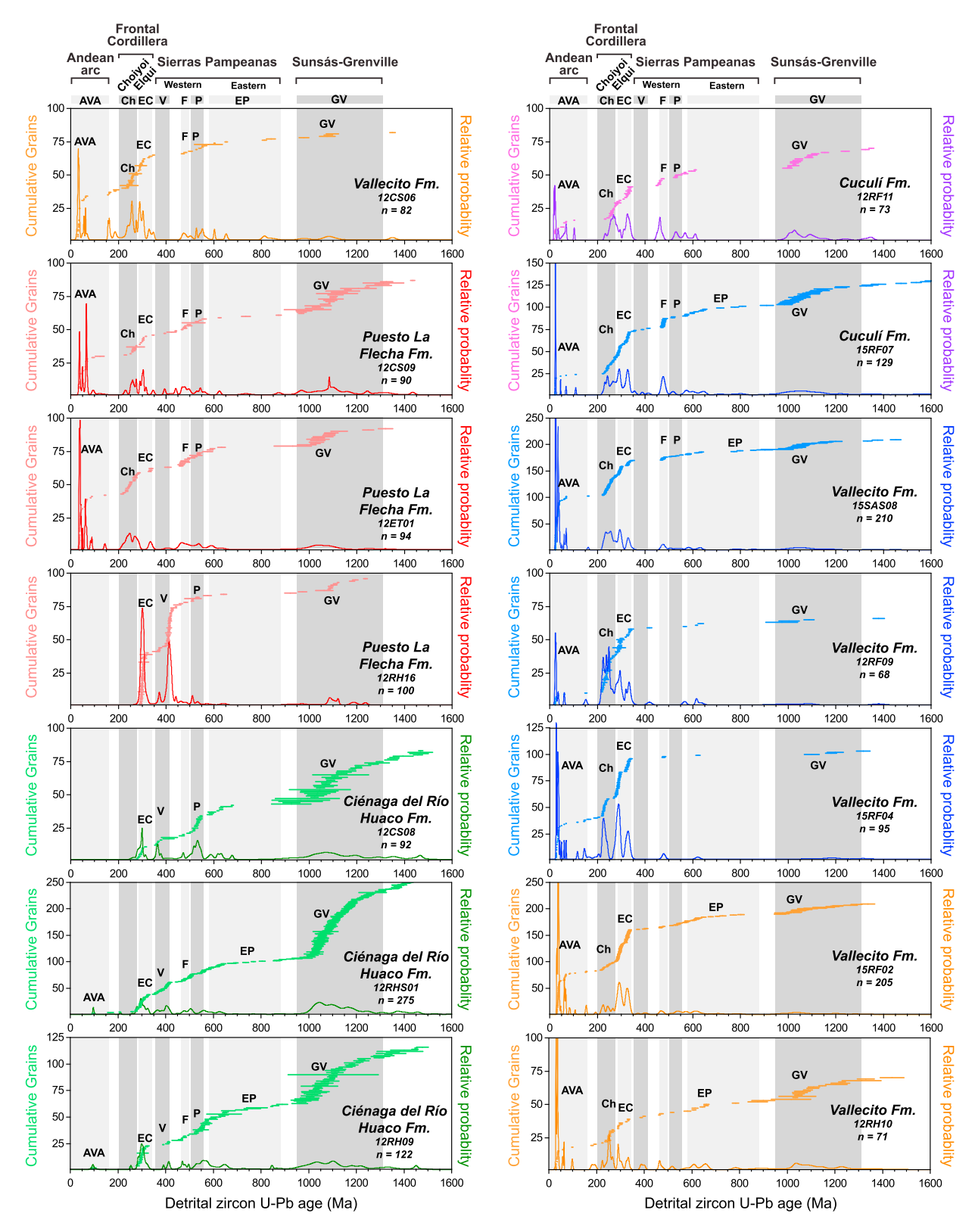


**Figure 7.** Detrital zircon U-Pb geochronology data from the Bermejo Basin. Relative probability distributions (lines) are shown at uniform scale for all samples. Cumulative number of analyzed grains (*n*) are shown as individual horizontal bars, with bar widths representative of 2σ uncertainty. Gray windows represent generalized age range of possible igneous sources following *Fosdick et al.* [2015], and references therein: AVA = Andean volcanic arc, Ch = Choiyoi, EC = Elqui Complex (Colangüil batholith), EP = Eastern Sierras Pampeanas, F = Famatinian arc, GV = Grenville, P = Pampean orogen, and SV = Sierra Velasco. Sample locations, analytical data, and U-Pb Concordia plots are reported in the supporting information.

analysis of the youngest component indicates an age of  $93.6 \pm 7.3$  Ma (n = 2). Sample 12RHS01 from a stratigraphically equivalent level to 12RH09 (Figure 3) generated a similar age distribution (n = 275) and a MDA  $95.0 \pm 2.8$  Ma (n = 3). Sample 12CS08 yielded zircon U-Pb ages between 264 and 3107 Ma (n = 92). Major age groups are 495-555 Ma and 780-1490 Ma, with lesser ages between 270-305 Ma, 355-390 Ma, and 575-645 Ma (Figure 7). A MDA was not calculated on this sample, since its direct outcrop correlation to other Cretaceous zircon-bearing strata (i.e., 12RHS01 and 12RH09) preclude a Permian age as suggested by the youngest zircons.

### 3.2.2.2. Puesto La Flecha Formation

Sample 12ET01 from the top of the Puesto La Flecha Formation in the El Templo section yields ages between 36 and 2850 Ma (n = 94). The majority of the analyzed zircons are between 38 and 44 Ma, with less pronounced ages between 60–70 Ma, 225–290 Ma, 440–615 Ma, and 945–1150 Ma (Figure 7). MDA analysis of the youngest component is 37.3  $\pm$  0.5 Ma (n = 26). Euhedral zoned prismatic zircon extracted from a minimally reworked airfall volcanic tuff (12ET02) yielded an error-weighted mean age of 37.4  $\pm$  1.0 Ma (n = 19), which we interpret as the eruptive age of the tuff. Sample 12CS09 from the top of the Puesto La Flecha Formation in the Ladrillos Rojos section yields ages between 34 and 2920 Ma (n = 90). The majority of the analyzed zircons are Cenozoic, with two dominant age groups between 34–50 Ma and 58–73 Ma, with lesser pronounced age components from 460–510 Ma to 930–1380 Ma (Figure 7). MDA analysis of the youngest component is 36.8  $\pm$  1.7 Ma (n = 5) (Figure 4). Sample 12RH16, collected from brick red planar cross-stratified deposits in the El Dique section, yields detrital zircon U-Pb ages between 293 and 2677 Ma (n = 100). Prominent ages range from 280–350 Ma to 390–480 Ma and a minor component between 1070 and 1130 Ma (Figure 7). MDA was not calculated from this sample due to the absence of young zircons of plausible depositional age.

# 3.2.2.3. Vallecito Formation

Six samples from the lower Vallecito Formation were analyzed. Sample 12CS06 is from the base of formation in the Ladrillos Rojos section and yields zircon U-Pb ages from 27 to 1350 Ma (n = 82). Prominent age groups are 27–45 Ma, 220–315 Ma, with minor components at 540–460 Ma, and 1040–1115 Ma (Figure 7). MDA analysis of the youngest component is 32.6 ± 1.5 Ma (n = 10). Sample 12RH10 was collected at the base of the unit in the El Dique section and produced a low zircon yield. Measured zircon U-Pb ages range from 29 to 2180 Ma (n = 71). Conspicuous age clusters include 29–40 Ma, 241–274 Ma, 850–1300 Ma, and with lesser component of ages between 285–301 Ma and 640–670 Ma (Figure 7). MDA analysis of the youngest age component is 30.1 ± 0.5 Ma (n = 5).

In the Río Francia area, 15RF02 was collected from the top of brown trough cross-bedded sandstone and yielded zircon U-Pb ages from 28 to 2068 Ma (n=205). Prominent age ranges are from 27–42 Ma, 59–70 Ma, 215–350 Ma, 515–645 Ma, 925–1255 Ma, and lesser amounts between 150–155 Ma and 450–480 Ma (Figure 7). MDA analysis of the youngest component is  $30.0 \pm 0.7$  Ma (n=9). Upsection, 15RF04, collected from the base of an orangish brown planar cross-bedded sandstone, yielded zircon U-Pb ages from 26 to 1730 Ma (n=95). Prominent zircon ages are from 26–40 Ma, 215–245 Ma, 265–305 Ma, 310–345 Ma, and lesser amounts between 475–622 Ma and 1100–1730 Ma (Figure 7). MDA analysis of the youngest component is  $28.0 \pm 0.5$  Ma (n=9).

Upsection in the Río Francia section, 12RF09, also had low zircon yield, and U-Pb dated zircons range in age from 22 to 2321 Ma (n = 68). Prominent age groups are 22–29 Ma, 210–295 Ma, and 315–345 Ma (Figure 7). MDA analysis of the youngest component is 25.4  $\pm$  1.3 Ma (n = 7). Sample 15RF07, collected from within an orangish brown planar cross-bedded sandstone, yielded zircon U-Pb ages from 23 to 2618 Ma (n = 129). Prominent age groups range between 21–27 Ma, 225–345 Ma, 460–495 Ma, 930–1225 Ma, and lesser amounts between 560 and 655 Ma (Figure 7). MDA analysis of the youngest component is 23.4  $\pm$  0.3 Ma (n = 12). Sample 15SAS08, collected from the top of the Vallecito Formation in the Ladrillos Rojos section (n = 210), contains similar ages and the youngest cluster MDA of 24.6  $\pm$  0.2 Ma (n = 44 grains).

# 3.2.2.4. Cuculí Formation

A single sample from the base of Cuculí Formation was collected for comparison with the underlying strata. Sample 12RF11 yielded zircons ranging in U-Pb age from 17 to 2858 Ma (n = 73). Most grains fall within populations of 17–26 Ma, 51–73 Ma, 245–296 Ma, 304–347 Ma, 452–544, and 990–1120 Ma (Figure 7). Prominent age populations are nearly identical to the underlying Vallecito Formation, with appearance of both Pampean sources and Grenville. MDA analysis of the youngest component is  $18.4 \pm 2.8$  Ma (n = 2 grains).



# 4. Interpretations

# 4.1. Revised Timing of Upper Cretaceous-Eocene Sedimentation

Detrital geochronology of magmatically derived zircon provides several important revisions to the basin chronology, with implications for basin tectonics and paleogeography as discussed below (Figure 8). First, our data present the first radiometrically dated Upper Cretaceous sedimentary units within the Argentine Precordillera and Bermejo Basin at this latitude. Our observations of the CRH corroborate those of *Limarino et al.* [2000] who interpreted a coarse-grained braided stream system that transitioned over time into a mean-dering river system. Deposition of the Ciénaga del Río Huaco Formation at the Huaco Anticline occurred as recently as Cenomanian-Turonian time (~93–95 Ma), though lack of young zircons from the basal CRH hampers our knowledge of the onset of this sedimentation phase. Others have previously demonstrated an Early Cretaceous sanidine K-Ar age (~117 Ma) from volcanic-rich deposits in the CRH in the La Troya Basin farther north (Figure 1b) [*Tedesco and Limarino*, 2007]. These radiometric dates both corroborate and refine the Cretaceous depositional age—based on ostracod and palynomorph assemblages [*Limarino et al.*, 2000]—for the ancestral Ciénaga del Río Huaco Formation river system. *Reat* [2016] reports a maximum depositional age of ~65.3 Ma from the transitional base of the overlying Puesto La Flecha Formation, suggesting a long-lived depocenter during Cretaceous time.

Based on our revised stratigraphy, we interpret the upper CRH of *Limarino et al.* [2000] to be the Puesto La Flecha Formation, based on the depositional change to lacustrine environment of deposition, different provenance, and substantially younger timing of sedimentation. New detrital geochronology from *Reat* [2016] documents a Paleocene maximum depositional age for the base of the Puesto La Flecha Formation. Our data from both interbedded volcanic ash and youngest zircon age clusters from sandstones in the thin-bedded evaporative lacustrine strata confirm the age of the upper Puesto La Flecha Formation to be ~37–33 Ma. An Eocene volcanic source of grains and interbedded volcanic ash are consistent with volcanic and hypabyssal diorite and granodiorite intrusions dated by *Bissig et al.* [2001] who report biotite and horn-blende <sup>40</sup>Ar/<sup>39</sup>Ar plateau ages between ~30 and 36 Ma. Although *Jordan et al.* [1993] suggested that the lower part of the red bed unit at El Fiscal may be pre-Cenozoic [*Limarino et al.*, 1987; *Peréz et al.*, 1993], more recent work has linked this unit to Oligocene-Miocene. Together, these new age constraints indicate very low rates of sediment accumulation and basin subsidence (see section 4.3 below) within a clastic-evaporative lake setting during Paleogene time.

The prevalence of syndepositional volcanic grains in our study provides robust depositional ages for the onset of eolian conditions. In the northern Bermejo Basin in the Huaco area, deposition of the Vallecito Formation occurred by at least ~33–30 and up until 18 Ma (Figure 3). Farther south near the Río Francia area (Figure 1), initiation of eolian sedimentation is broadly coeval but may be as young as ~23 Ma, based on MDA estimates from the sections. Here fluvial sedimentation began at ~18 Ma (Cuculí Formation) (Figure 8).

# 4.2. Synthesis of Provenance Data Sets

The petrographic and geochronologic data sets characterize first-order signatures of sediment provenance. In all sections the CRH is enriched in monocrystalline quartz and high-grade metamorphic lithic grains (Figure 6), suggesting deeply eroded recycled orogen and craton interior sources, consistent with Sierras Pampeanas sources and a lesser contribution from the Pennsylvanian-Permian Colangüil batholith and Cretaceous magmatic arc (Figure 10). The sandstones are both compositionally and texturally mature with low feldspar content, signifying erosion and weathering of stable source areas. We note that our data yielded slightly higher amount of lithic grains compared to *Ariza* [2009], who reported QFL provenance fields of basement uplift/craton interior for the CRH. The sandstone composition of the Puesto La Flecha Formation changes upsection from dominantly *Qm* and high-grade metamorphic lithic grains, compositionally similar to the underlying CRH, to higher proportions of volcanic and sedimentary lithic grains. The appearance of Cenozoic zircons and abundant intermediate lathwork volcanic and sedimentary lithics supports a sedimentary source in the Andean Arc. Upsection, the eolian sandstones of the Vallecito Formation, contains higher proportions of feldspar and lithic grains and reduced amount of monocrystalline quartz and metamorphic lithics. However, we note that both the relative proportions of feldspar to total lithics and the type of lithic grains vary across samples, likely representing local sources for wind-derived detritus.

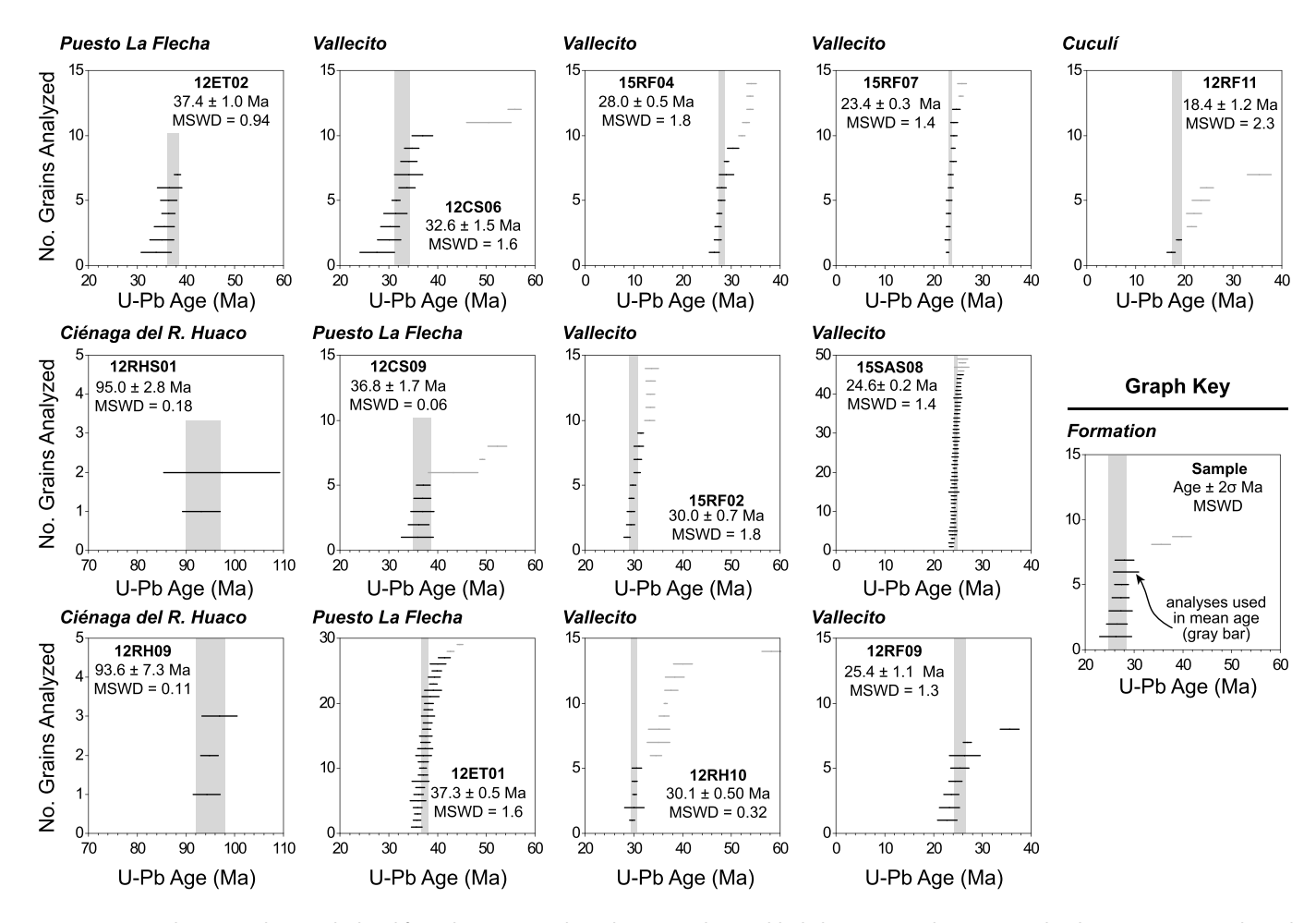


**Figure 8.** Maximum depositional ages calculated from the youngest detrital zircon U-Pb ages (black data points only). Error-weighted mean ages (vertical gray bars,  $2\sigma$ ) are calculated from age clusters of concordant grains with overlapping ages at  $2\sigma$  uncertainty.

# 4.3. Paleogene Basin Subsidence Mechanism

We performed 1-D backstripping analysis on the Ladrillos Rojos composite section to evaluate changes in subsidence rate over time near the Huaco study area and test the hypothesis that the fluvial and lacustrine strata are compatible with flexurally driven subsidence (Figure 9). Alternatively, Eocene strata may preserve subsidence due to residual thermal or postrifting subsidence [Ramos and Aleman, 2000]. Here backstripping takes into account compaction of sedimentary infill for the mudstone and sandstone lithologies using an Athy depth-porosity relationship to calculate the residual tectonic subsidence from total subsidence [van Hinte, 1978; Allen and Allen, 2013]. All input stratigraphic data and modeling parameters are reported in the supporting information. Backstripping results show very low (<0.003 mm yr<sup>-1</sup>) tectonic subsidence rates during Cretaceous-Paleocene time, with accelerating subsidence (>0.02 mm yr<sup>-1</sup>) beginning in late Eocene time and culminating in highest flexural subsidence during Miocene deposition near Huaco (Figure 9) [Johnson et al., 1986; Cardozo and Jordan, 2001]. The shape of the subsidence curve (upward convex) and the accelerating rates beginning in the Paleocene suggest a flexural subsidence mechanism. Topographic loading from the Frontal Cordillera is a permissible source of flexural subsidence, based on a first-order elastic model of elastic flexure of the retroarc lithosphere (supporting information). Based on the new chronological constraints and similar sediment source signatures of the Puesto La Flecha and Vallecito Formations, we further suggest that these sedimentary strata were part of the same distal foreland basin system formed as a result of flexural and accelerating subsidence during progressive Andean topographic construction of the Frontal Cordillera.

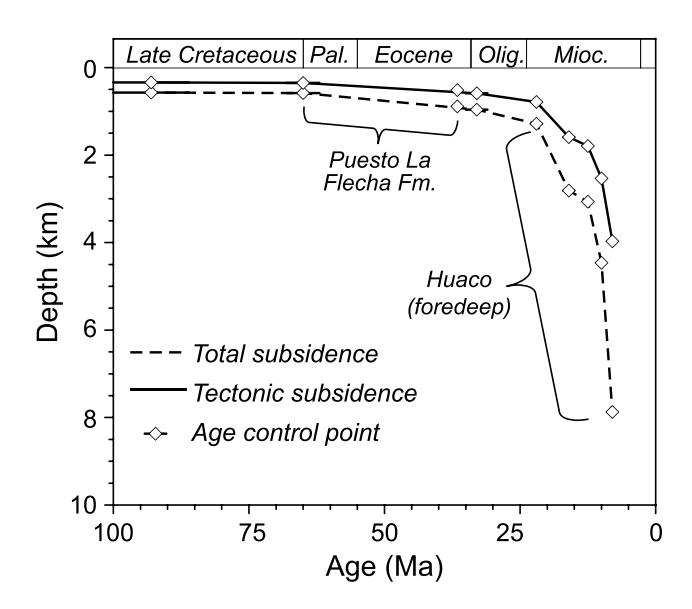


**Figure 9.** Calculated sediment accumulation and tectonic subsidence for the Huaco area using new stratigraphic and chronological data. Tectonic subsidence rate increases during deposition of the Puesto La Flecha and Vallecito Formations and culminates with Miocene Huaco foredeep deposition. See text for discussion and supporting information for modeling methods.

# 5. Discussion

# 5.1. Tectonic Significance of Newly Recognized Upper Cretaceous-Eocene Sedimentation

# 5.1.1. Late Cretaceous Retroarc Basin Sedimentation

Cenomanian-Turonian 93 Ma) Ciénaga del Río Huaco Formation preserves a through-going coarse clastic fluvial stream at least 25 km wide, with predominantly southward sediment dispersal indicators. This fluvial network transferred lithic arkosic to arkosic detritus derived from northern recycled basement sources into the basin [Reat, 2016]. The marked lack of Choiyoi zircons and volcanic detritus, diagnostic signals of the Frontal Cordillera located to the west (Figure 7), is consistent with limited transverse sediment input. Rather, the fluvial sedimentary system was dominated

by well-rounded quartzite and aphanitic cobbles in an arkosic matrix. The uniform detrital zircon U-Pb age distributions from multiple locations within the fluvial system point to a well-mixed axial sediment routing system between the Río Francia and Huaco areas that received sediment from northern and eastern high-lands—with key provenance connections to the 900–1200 Ma Sunsás magmatic belt [Bahlburg et al., 2009], the 360–320 Ma Sierra Velasco [Grosse et al., 2009], the 525–550 Ma Pampean Arc [Ramos, 2009], with lesser input from western tributaries that appear to have tapped the Pennsylvanian-Permian Colangüil batholith. These igneous sources are consistent with a recycled orogen sediment provenance, with Grenville/Sunsás age zircon or other recycled Pampean sources [e.g., Fosdick et al., 2015]. We note similar detrital zircon U-Pb age distributions in the Fiambalá Basin and surrounding highlands [Safipour et al., 2015], suggesting compatible northern sources for the CRH detritus.

The presence of an Upper Cretaceous axially drained fluvial system through the protoforeland has important implications for sediment routing along the Andean system, during a time in basin history thought to be tectonically quiescent at this latitude and position, even with ongoing subduction and arc magmatism in the west and intracontinental rifting to the east [Ramos and Aleman, 2000]. We interpret these deposits to reflect a combination of high-energy sediment flux of coarse-grained detritus and low subsidence rate, leading to restricted deposition and facilitating bypass to a southern depocenter. Remnant rift-related topography from the Cuyo rifts may have further funneled sediment southward [Giambiagi and Martinez, 2008]. The presence of Upper Cretaceous-Paleogene coarse-grained fluvial deposits of the Papagayos Formation near Mendoza [Yrigoyen, 1993; Folguera et al., 2001] may point to a more complex basin paleogeography between Mesozoic rifted depocenters and younger sedimentation patterns.

# 5.1.2. Eocene-Oligocene Basin Reorganization

The presence of newly recognized Paleogene deposits in the northern Bermejo Basin necessitates a reevaluation of the tectonic controls on basin subsidence and their relationship to other age-equivalent units during their deposition. The Puesto La Flecha Formation detrital zircon U-Pb signature heralds the appearance of Andean zircons, Choiyoi Group, Carboniferous Elqui complex, and a noticeable paucity of Pampean zircons compared to the CRH deposits (Figure 7). Upsection, the framework sandstone composition shifts from arkosic to feldspathic litharenite/litharenite, consistent with higher proportion of intermediate volcanic lithic grains. Taken together, we interpret the prevalence of Andean Arc and Choiyoi zircons and abundance of volcanic lithics as clear evidence that the Frontal Cordillera and arc highlands became a primary source of the retroarc foreland basin detritus by late Eocene time. We suggest that such a provenance shift from

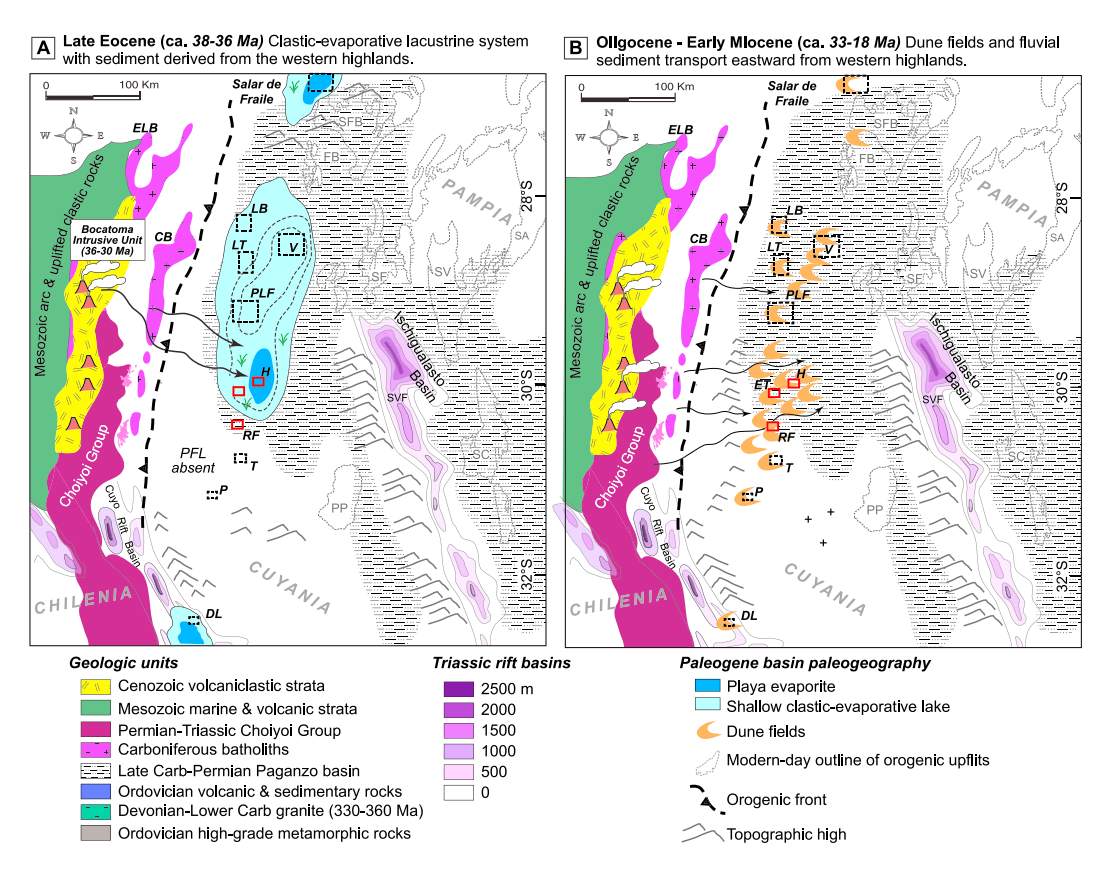


**Figure 10.** Paleogeographic reconstruction of the Andean retroarc depocenter, accounting for ~90 km of palinspastically restored Miocene shortening across the Argentine Precordillera [*Allmendinger and Judge*, 2014]. (a) Late Eocene time, showing a shallow clastic-evaporative lacustrine system with sediment derived from the western highlands. (b) Oligocene-early Miocene time, showing dune fields and fluvial sediment transport eastward from western highlands. Stratigraphic sections or depocenters discussed in the text: DL = Divisadero Largo, ET = El Templo, HA = Huaco Anticline, FB = Fiambala Basin, LB = Laguna Brava, LT = La Troya, P = Pachaco, PLF = Puesto La Flecha, RF = Río Francia, T = Talacasto, and V = Vinchina. Igneous source areas in the Frontal Cordillera are as follows: CB = Colangüil batholith, ELB = Elqui Limari batholith, and Carboniferous batholiths; and Cenozoic volcanics are from *Mpodozis and Kay* [1992] and *Bissig et al.* [2002], respectively. Sierras Pampeanas uplifts (modern outlines of exposed blocks): PP = Pie de Palo, SA = Sierra Aconquija Sierra de Ambato, SC = Sierra Chepes, SdF = Salar de Fraile, SF = Sierra de Famatina, SFB = Sierra de Fiambala; SM = Sierra de Maz, SVF = Sierra de Valle Fertil, and SV = Serra Velasco. Triassic rift basin contours from *Giambiagi and Martinez* [2008].

northern to western sources, coupled with a shift in environment to an evaporative clastic lacustrine system, reflects both uplift of western sources and capture of the ancestral CRH river system via topographic damming from paleotopography [e.g., *Walcek and Hoke*, 2012]. Where observed, the Puesto La Flecha Formation is thickest in the Vinchina Basin area (Figure 10), consistent with higher magnitude of subsidence in the north, and thinning southward in the Bermejo Basin. During the Eocene-Oligocene transition, sediments record increasing Choiyoi input upsection over time, as well as increasing Choiyoi sediment input from north to south (Figure 7). We also note that the El Templo and Río Francia Puesto La Flecha Formation sources have a stronger Andean signature, consistent with their more proximal positions. In contrast, the Puesto La Flecha and Vallecito Formations in the Huaco area have higher proportions of Grenville/Sunsás zircons that may reflect a combination of reworking of the exposed Carboniferous-Permian Paganzo Basin deposits [e.g., *Fosdick et al.*, 2015].

Our results indicate a major change in both sediment provenance and depositional environment during Paleocene-Eocene time, with inception of an evaporative fluvial-lacustrine system that received sediments from a dominantly Andean-derived source (i.e., Frontal Cordillera and magmatic arc) (Figure 10). The Puesto La Flecha Formation in the Huaco area (this study) exhibits similar lithofacies as those reported in the ~38–34 Ma Laguna Brava Formation to the north (Figure 1) [Vizán et al., 2013]. Based on sedimentological similarity, we propose that these units are stratigraphically equivalent and genetically related. We further

postulate that the Puesto La Flecha Formation in the Vinchina area, situated laterally along strike between the Laguna Brava section and the northern Bermejo Basin, is likely as young as late Eocene as well. Although no numerical ages are available in the Vinchina-La Troya area, a pre-Oligocene age is permitted by turtle shells [De La Fuente et al., 2003].

Additionally, the Puesto La Flecha Formation shares similar lithological characteristics with the Paleogene Divisadero Largo Formation near Mendoza (Figure 1), a unit composed of multicolored fine-grained sandstone, siltstone, and mudstone; interbedded gypsum; and capping eolian deposits [*Yrigoyen*, 1993; *Irigoyen et al.*, 2000]. The provenance and depositional age for Divisadero Largo Formation are not radiometrically defined, but vertebrate fossils suggest an upper Eocene to lower Miocene age. Taken together, these regional stratigraphic correlations may point to the existence of a more extensive series of Eocene topographically partitioned, evaporative fluvial-lacustrine depocenters spanning >300 km along the eastern margin of the Andes (Figure 10). The lateral extent of the Puesto La Flecha Formation and equivalent strata suggests a broad region of shallow basins with low tectonic subsidence and sediment accumulation rates.

The striking provenance similarity to overlying Oligocene-Miocene foreland basin fill leads to our preferred interpretation that the Eocene deposits reflect incipient stages of distal foreland sedimentation that preceded the main phase of Oligocene-Miocene proximal foredeep deposition and growth of the Argentine Precordillera [Jordan et al., 2001] (Figure 10b). Along the Andean margin, the transition to compressive Andean cycle began during the Late Cretaceous [Mpodozis and Ramos, 1990], though the reported timing of upper plate shortening and thickening is highly variable and subject to the dating of foreland basin deposits [Kley et al., 1999; DeCelles et al., 2011; Giambiagi et al., 2012]. Thus, the southern central Andes may have resided in a prolonged setting of postrifting thermal relaxation [Ramos and Aleman, 2000], prior to construction of a full-fledged fold-thrust belt and foreland basin system. The onset of foreland basin subsidence at this latitude has long been cited as late Oligocene-early Miocene, based on the thick accumulation of foredeep strata in the Bermejo Basin [Jordan et al., 2001]. Although the Oligocene-Miocene phase of Bermejo Basin sedimentation reflects the most recent phase of major mountain building and crustal shortening during Andean growth [Jordan et al., 2001], we propose that the underlying fluvial and lacustrine strata of the Puesto La Flecha Formation, with its Andean-derived detritus, represent an incipient phase of foredeep sedimentation and topographic growth in the Frontal Cordillera. Further recognition of Eocene foreland basin deposition has been complicated by clear evidence of Paleogene intraarc extension in the Valle del Cura [Litvak et al., 2007; Winocur et al., 2014], though lateral and temporal heterogeneity in stress conditions across localized extensional intraarc and compressional retroarc domains during Cordilleran-type orogenesis is possible [DeCelles, 2004; Busby, 2012; Horton and Fuentes, 2016]. Arc magma geochemistry from the southern central Andes depicts multiple phases of retroarc extension since Late Cretaceous time, with a notable Iull of extension from middle Eocene to early Oligocene [Jones et al., 2016]. Furthermore, new work in the Frontal Cordillera at ~28.5°S documents contractional deformation at ~46-44 Ma prior to localized extension [Rossel et al., 2016], which may signal an important phase of structural development in the Andes.

Our interpretation of Paleogene retroarc foreland sedimentation in the southern central Andes offers an important orogen-scale comparison. Specifically, evidence of retroarc foreland sedimentation that is coeval with Paleocene-Eocene activity in the central Andes of northwestern Argentina [DeCelles et al., 2011; Carrapa et al., 2012], where substantial upper plate lithospheric shortening has occurred, suggests synchronous basin processes despite widely variable magnitude of lithospheric shortening [Kley et al., 1999; Hilley and Coutand, 2010] and complexity of upper plate structural inheritance [Giambiagi et al., 2003; Carrapa and DeCelles, 2015]. In contrast, the Paleogene sedimentation record south of 34°S, in the Neuquén basin, is marked by a major depositional hiatus interpreted to reflect reduced plate coupling and neutral or extensional conditions in the retroarc area [Horton and Fuentes, 2016]. Paleogene sedimentation in the northern Bermejo Basin may point to a northern shift in flexural subsidence and sedimentation.

#### 5.1.3. Diachronous Onset of Aridification and Eolian Deposition

The presence of arid conditions has been an important paleoenvironmental indicator in orographic effects in major orogenic systems [e.g., *Alonso et al.*, 2006; *Ruskin et al.*, 2011; *Quade et al.*, 2015]. Our data better resolve the timing of aridification and eolian conditions within the southern central Andes and identify the oldest dated eolian deposits within the Andean retroarc region. Regional evaporative conditions were established in the retroarc foreland basin by ~37 Ma, predating the major global Eocene-Oligocene

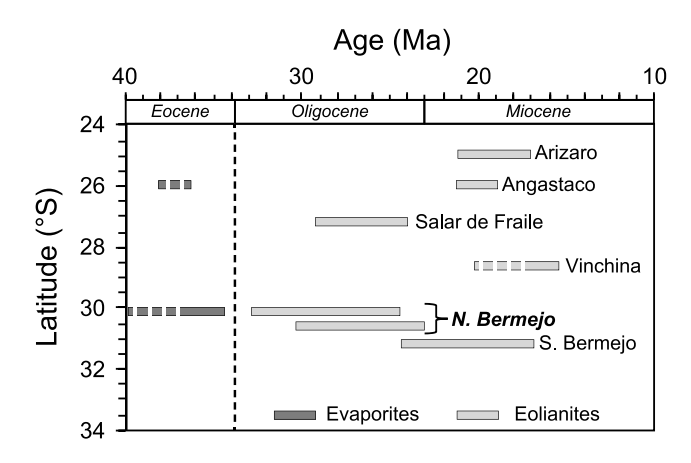


**Figure 11.** Available chronology of evaporites and eolian deposition in the southern Central Andean retroarc basin, between 24 and 32°S. Units include the Vizcachera Formation, Arizaro Basin [*DeCelles et al.*, 2015b], lower Angastaco Formation [*DeCelles et al.*, 2011; *Carrapa et al.*, 2012], Vallecito Formation, northern Bermejo Basin (this study), southern Bermejo Basin [*Levina et al.*, 2014], and Vinchina Basin [*Ciccioli et al.*, 2010].

shift toward a cool and arid climate (Figure 11). Aridification appears to be coeval with a reorganization of the sediment routing system as the Frontal Cordillera and Andean Arc in the west became dominant sediment sources to the foredeep (Figures 7 and 10b). Therefore, we propose that topographic uplift of these western ranges also restricted any Pacific-derived winter precipitation from the paleo-Westerlies midlatitude storms [e.g., Karnauskas Ummenhofer, 2014] from reaching the low-elevation Bermejo retroarc basin.

The timing of evaporative conditions in the Bermejo Basin compares favorably with the well-documented

record of basin aridification observed on the Puna Plateau ~27.2°S, where the Quiñoas Formation of the Salar de Fraile evaporites was deposited ~37–32 Ma [Carrapa et al., 2012; Canavan et al., 2014]. Farther north on the Andean Plateau, north of 26°S latitude, episodically dry conditions were in place by ~37 Ma during deposition of the lower Geste Formation [Carrapa and DeCelles, 2008]. The oldest playa deposits become progressively younger to the west, attributed to the eastward migration of surface uplift and orographic blocking of prevailing eastern moisture sources (see Quade et al. [2015] for a summary). In contrast, the Bermejo Basin—which also records hydrologically closed, evaporative conditions at ~37 Ma—resides off of the plateau and serves as a low-elevation (<1000 m) benchmark for paleoclimatic and environmental conditions in the leeward position of paleo-Westerlies during evolving Andean deformation.

We synthesize our data with the available chronology of Cenozoic evaporite and eolian deposition spanning ~32-25 °S (Figure 11) and note a northward younging of late Oligocene-early Miocene inception of eolian conditions. By early Miocene time, the Andean retroarc foredeep encompassed an extensive network of dune fields. Farther south in the southern Bermejo Basin, initiation of eolian sedimentation at Pachaco and Talacasto localities occurred between ~24 and 20 Ma [Levina et al., 2014], although in these areas, the preeolian Puesto La Flecha and CRH formations (or equivalents) are not present. There, eolian strata are deposited atop Paleozoic rocks. These paleogeographic relationships corroborate paleoerosion rates and geomorphic findings that document substantial paleorelief in the Precordillera near the present Mendoza-San Juan border prior to 10 Ma [Walcek and Hoke, 2012]. In the Vinchina Basin at ~28.7°S, robust constraints on the inception of eolian Vallecito Formation are lacking, but eolian conditions are replaced by fluvial sedimentation by ~15.4 Ma [Ciccioli et al., 2010]. Near 25-26°S, in the Puna Plateau region, the first evidence of eolian conditions is in early Miocene time with ~21 Ma deposition of the Vizcachera Formation in the Arizaro Basin (Figure 1) [DeCelles, et al., 2015b]. Other evidence of eolian deposition comes from the early Miocene lower Angastaco Formation in the Angastaco Basin [DeCelles et al., 2011; Carrapa et al., 2012]. Broadly, these findings suggest a first-order northward expansion of eolian dune conditions starting at ~33 Ma in the Bermejo Basin with a fluvial system resuming and dominating starting at ~18 Ma (Río Francia) and ~16 Ma (Huaco area). The expansion of dune fields beginning at ~32 Ma in the northern Bermejo Basin likely reflects enhanced aridification related to global climate optima during the early Oligocene [Zachos et al., 2008].

# 6. Conclusions

Integrated sedimentology, geochronology, provenance analysis, and flexural modeling of pre-Oligocene strata in the Bermejo Basin reveal siliciclastic-evaporative fluvial, lacustrine, and eolian environments indicating an initial phase of Oligocene-Miocene construction of the Frontal Cordillera and Argentine

Precordillera. We report the first radiometric dates from detrital zircons collected in the Ciénaga del Río Huaco Formation that confirm a Late Cretaceous maximum depositional age from strata previously mapped as Permian. Detrital zircon U-Pb ages of ~38–37 Ma from the overlying red beds further support sedimentation prior to onset of Oligocene eolian deposition and extend back the incipient foreland basin record into at least Eocene time. Backstripping calculations of the basin infill yield accelerating tectonic subsidence rates beginning in Eocene time, compatible with a basin paleogeography characterized by foredeep deposition, with fluvial connectivity to the Frontal Cordillera and Andean volcanic arc. Maximum depositional ages of the overlying Vallecito Formation suggest an early Oligocene or younger onset of eolian conditions at 30°S. A regional synthesis of Cenozoic eolian dune deposits spanning ~32-25°S suggests a northward younging of inception of eolian conditions; by early Miocene time, the Andean retroarc foredeep encompassed an extensive network of dune fields. Our findings revise the timing of a condensed Paleogene sedimentation history and suggest that the Upper Cretaceous and Paleogene strata are genetically related to the Andean phase of contractional deformation. More specifically, the Eocene Puesto La Flecha Formation and stratigraphic correlatives reflect existence of discontinuous topography that received sediment shed primarily from the Frontal Cordillera and Andean magmatic arc during the early phase of Paleogene structural growth of the central Andes.

#### Acknowledgments

This research was supported by the U.S. National Science Foundation Grant EAR-1049605 awarded to J.C.F. and the Robert R. Shrock Foundation at Indiana University. Precipitation and wind circulation data shown in Figure 1 and chronology data of eolian deposits summarized in Figure 11 are available in the supporting information. We thank Andrea Stevens, Teresa Jordan, Brian Mahoney, Julieta Suriano, and Brian Horton for fruitful discussions of Andean geology. The Arizona LaserChron Center (supported by NSF-EAR Award 1338583) provided expert analytical assistance. We kindly acknowledge project PDTS (UNSJ) E985 and the Secretaría de Ambiente of the San Juan Province Government and personnel for their permission to conduct fieldwork in the Ciénaga del Río Huaco Preserve, Argentina. The Universidad Nacional de San Juan generously provided field support during a 2012 field campaign. We thank Laura Giambiagi and an anonymous reviewer for their constructive suggestions that enriched the clarity of the study.

# References

- Allen, P. A., and J. R. Allen (2013), Basin Analysis: Principles and Application to Petroleum Play Assessment, 3rd ed., Wiley-Blackwell, Chichester, England.
- Allmendinger, R. W., and P. A. Judge (2014), The Argentine Precordillera: A foreland thrust belt proximal to the subducted plate, *Geosphere*, 10(6), 1203–1218.
- Allmendinger, R. W., D. Figueroa, D. Snyder, C. Mpodozis, and L. Isacks (1990), Foreland shortening and crustal balancing in the Andes at 30°S latitude, *Tectonics*, *9*(4), 789–809, doi:10.1029/TC009i004p00789.
- Alonso, R. N., et al. (2006), Tectonics, climate, and landscape evolution of the southern central Andes: The Argentine Puna Plateau and adjacent regions between 22 and 30oS, in *The Andes: Active Subduction Orogeny*, edited by O. Oncken et al., pp. 265–283, Springer, Berlin, Heidelberg.
- Alvarado, P., and M. Araujo (2011), La importancia de las redes sísmicas locales en la caracterización de la sismicidad cortical más peligrosa de la Argentina, in *Internacional Conference in Honour of Ing. Alberto Giesecke M*, pp. 57–72, Lima, Perú.
- Alvarado, P., S. Beck, and G. Zandt (2007), Crustal structure of the south-central Andes Cordillera and back arc region from regional waveform modelling, *Geophys. J. Int.*, 170, 858–875.
- Ammirati, J. B., S. Pérez Luján, P. Alvarado, S. Beck, S. Rocher, and G. Zandt (2016), High-resolution images above the Pampean flat slab of Argentina (31–32°S) from local receiver functions: Implications on regional tectonics, *Earth Planet. Sci. Lett.*, 450, 29–39.
- Ariza, J. P. (2009), Caracterización sedimentológical y paleoambiental d la Formación Patquía (Pérmico) en el área de la Ciénaga del Río Huaco, Precordillera Central de San Juan Departamento Jáchal, Licenciatura en Geología, Universidad Nacional de San Juan.
- Bahlburg, H., J. D. Vervoort, S. A. D. Frane, B. Bock, C. Augustsson, and C. Reimann (2009), Timing of crust formation and recycling in accretionary orogens: Insights learned from the western margin of South America, *Earth Sci. Rev.*, 97, 215–241.
- Barnes, J. B., T. A. Ehlers, N. Insel, N. McQuarrie, and C. J. Poulsen (2012), Linking orography, climate, and exhumation across the central Andes, *Geology*, 40, 1135–1138.
- Bissig, T., J. K. W. Lee, A. H. Clark, and K. B. Heather (2001), The Cenozoic History of Volcanism and Hydrothermal Alteration in the Central Andean Flat-Slab Region: New 40 Ar- 39 Ar Constraints from the El Indio–Pascua Au (-Ag, Cu) Belt, 29°20′–30°30′ S, Int. Geol. Rev., 43, 312–340.
- Bissig, T., A. H. Clark, and J. K. W. Lee (2002), Miocene landscape evolution and geomorphologic controls on epithermal processes in the El Indio-Pascua Au-Ag-Cu belt. Chile and Argentina. *Econ. Geol.* 97, 971–996.
- Bookhagen, B., and M. R. Strecker (2012), Spatiotemporal trends in erosion rates across a pronounced rainfall gradient: Examples from the southern Central Andes, *Earth Planet. Sci. Lett.*, 327–328, 97–110.
- Borello, A., and A. Cuerda (1968), Grupo Río Huaco (Triásico), San Juan, Com. Investig. Científicas la Prov. Buenos Aires, 7, 3-15.
- Bracaccini, O. (1946), Contribución al conocimiento geológico de la Precordillera Sanjuanino-Mendocina, *Boletín Inf. Pet., 258*, 260–265. Busby, C. J. (2012), Extensional and Transtensional Continental ARC Basins: Case Studies from the Southwestern United States, in *Tectonics of*
- Sedimentary Basins: Recent Advances, edited by C. Busby and A. Azor, pp. 382–404, Blackwell Ltd., Chichester, England.
  Canavan, R. R., B. Carrapa, M. T. Clementz, J. Quade, P. G. DeCelles, and L. M. Schoenbohm (2014), Early cenozoic uplift of the Puna plateau, central Andes, based on stable isotope paleoaltimetry of hydrated volcanic glass, Geology, 42, 447–450.
- Cardozo, N., and T. Jordan (2001), Causes of spatially variable tectonic subsidence in the Miocene Bermejo Foreland Basin, Argentina, Basin Res., 13, 335–357.
- Carrapa, B., and P. G. DeCelles (2008), Eocene exhumation and basin development in the Puna of northwestern Argentina, *Tectonics*, 27, TC1015, doi:10.1029/2007TC002127.
- Carrapa, B., and P. G. DeCelles (2015), Regional exhumation and kinematic history of the central Andes in response to cyclical orogenic processes, *Geol. Soc. Am. Mem.*, 212, 201–213.
- Carrapa, B., J. Hauer, L. Schoenbohm, M. R. Strecker, A. K. Schmitt, A. Villanueva, and J. Sosa Gomez (2008), Dynamics of deformation and sedimentation in the northern Sierras Pampeanas: An integrated study of the Neogene Fiambala basin, NW Argentina, *Geol. Soc. Am. Bull.*, 120. 1518–1543.
- Carrapa, B., S. Bywater-Reyes, P. G. DeCelles, E. Mortimer, and G. E. Gehrels (2012), Late Eocene-Pliocene basin evolution in the Eastern Cordillera of northwestern Argentina (25°-26°S): Regional implications for Andean orogenic wedge development, *Basin Res.*, 24, 240-240.
- Caselli, A. (2002), Paleoenvironment and stratigraphic correlation of the Tertiary Puesto La Flecha Formation, La Rioja Province, Argentina, Actas del Congr. Geol. Argentino, 15, 679–683.

- Charrier, R., V. A. Ramos, F. Tapia, and L. Sagripanti (2014), Tectono-stratigraphic evolution of the Andean Orogen between 31 and 37 S (Chile and Western Argentina), Geol. Soc. London, Spec. Publ., 399, 13–61.
- Ciccioli, P. L., S. Ballent, A. M. Tedesco, V. Barreda, and C. O. Limarino (2005), Hallazgo de depósitos cretácicos en la Precordillera de La Rioja (Formación Ciénaga del Río Huaco), Rev. Asoc. Geol. Argent., 60, 122–131.
- Ciccioli, P. L., C. O. Limarino, S. A. Marenssi, A. M. Tedesco, and A. Tripaldi (2010), Estratigrafía de la cuenca de Vinchina (Terciario), Sierras Pampeanas, Provincia de la Rioja, *Rev. Asoc. Geol. Argent.*, 66, 146–155.
- Ciccioli, P. L., C. O. Limarino, S. A. Marenssi, A. M. Tedesco, and A. Tripaldi (2011), Tectosedimentary evolution of the La Troya and Vinchina depocenters (northern Bermejo Basin, Tertiary), La Rioja, Argentina, in *Cenozoic Geology of the Central Andes of Argentina*, edited by M. R. A. Salfity, J. A., pp. 91–110, SCS Publ., Salta, Argentina.
- Ciccioli, P. L., C. O. Limarino, R. Friedman, and S. A. Marenssi (2014), New high precision U-Pb ages for the Vinchina Formation: Implications for the stratigraphy of the Bermejo Andean foreland basin (La Rioja province, western Argentina), *J. South Am. Earth Sci.*, 56, 200–213. Cook, K. H. (2003), Role of continents in driving the Hadley cells. *J. Atmos. Sci.*, 60, 957–976.
- DeCelles, P. G. (2004), Late Jurassic to Eocene evolution of the Cordilleran thrust belt and foreland basin system, western U.S.A, Am. J. Sci., 304. 105–168.
- DeCelles, P. G., M. N. Ducea, P. Kapp, and G. Zandt (2009), Cyclicity in Cordilleran orogenic systems, Nat. Geosci., 2, 251–257.
- DeCelles, P. G., B. Carrapa, B. K. Horton, and G. E. Gehrels (2011), Cenozoic foreland basin system in the central Andes of northwestern Argentina: Implications for Andean geodynamics and modes of deformation, *Tectonics*, 30, TC6013, doi:10.1029/2011TC002948.
- DeCelles, P. G., G. Zandt, S. L. Beck, C. A. Currie, M. N. Ducea, P. Kapp, G. E. Gehrels, B. Carrapa, J. Quade, and L. M. Schoenbohm (2015a), Cyclical orogenic processes in the Cenozoic central Andes. *Geol. Soc. Am. Mem.*, 212, 459–490.
- DeCelles, P. G., B. Carrapa, B. K. Horton, J. McNabb, G. E. Gehrels, and J. Boyd (2015b), The Miocene Arizaro Basin, central Andean hinterland: Response to partial lithosphere removal?, *Geol. Soc. Am. Mem.*, 212, 359–386.
- Deichmann, U., and L. Eklundh (1991), Global digital data sets for land degradation studies: A GIS approach, *GRID Case Study Ser.*, 4, 24–27. De La Fuente, M. M., P. L. Ciccioli, C. O. Limarino, P. R. Gutierrez, and L. E. Fauqué (2003), Quelonios podocnemídidos en la Formación Puesto La Flecha (Oligoceno), Precordillera de La Rioja, Argentina, *Ameghiniana*, 40, 617–624.
- Dickinson, W. R. (1985), Interpreting provenance relations from detrital modes of sandstones, in *Provenance of Arenites*, edited by G. G. Zuffa, pp. 333–361, NATO Advanced Studies Inst., Dordrecht, Netherlands.
- Ducea, M. N., J. E. Otamendi, G. W. Bergantz, D. Jianu, and L. Petrescu (2015), The Ordovician Famatinian-Puna arc, *GSA Mem.*, *212*, 125–138. England, P., and P. Molnar (1990), Surface uplift, uplift of rocks, and exhumation of rocks, *Geology*, *18*, 1173–1177.
- Fernandez-Seveso, F., B. Aires, and A. J. Tankard (1995), Tectonics and stratigraphy of the late Paleozoic Paganzo Basin of western Argentina and its regional implications, AAPG Mem., 62, 285–301.
- Fiorella, R. P., C. J. Poulsen, R. S. Pillco Zolá, J. B. Barnes, C. R. Tabor, and T. A. Ehlers (2015), Spatiotemporal variability of modern precipitation  $\delta^{18}$ O in the central Andes and implications for paleoclimate and paleoaltimetry estimates, *J. Geophys. Res. Atmos.*, 120, 4630–4656, doi:10.1002/2014JD022893.
- Flemings, P. B., and T. E. Jordan (1990), Stratigraphic modeling of foreland basins: Interpreting thrust deformation and lithosphere rheology, *Geology*, 18, 430–434.
- Folguera, A., M. Etcheverria, P. Pazos, L. B. Giambiagi, J. M. Cortés, L. Fauqué, C. Fusari, and M. F. Rodriguez (2001), *Descripción de la Hoja Geológica Potrerillos (1:100.000)*, Subsecretaría de Minería de la Nación, Dirección Nacional del Servicio Geológico.
- Fosdick, J. C., B. Carrapa, and G. Ortíz (2015), Faulting and erosion in the Argentine Precordillera during changes in subduction regime: Reconciling bedrock cooling and detrital records, *Earth Planet. Sci. Lett.*, 432, 73–83.
- Furque, G., P. D. González, and M. F. Caballé (2003), Hoja Geológica 3169—II San José de Jáchal, 1:250,000, SEGEMAR Inst. Geol. y Recur. Miner., 259, 1–83.
- Garreaud, R. D., M. Vuille, R. Compagnucci, and J. Marengo (2009), Present-day South American climate, *Palaeogeogr. Palaeoclimatol. Palaeoecol.*, 281(3–4), 180–195.
- Gehrels, G. E., V. Valencia, and A. Pullen (2006), Detrital zircon geochronology by laser-ablation multicollector ICPMS at the Arizona Laserchron Center, in *From Geochronology: Emerging Opportunities, Paleontological Society Short Course*, vol. 12, edited by T. Olszewski, pp. 67–76. The Paleontological Society. Philadelphia. Pa.
- Giambiagi, L., and A. N. Martinez (2008), Permo-Triassic oblique extension in the Potrerillos-Uspallata area, western Argentina, J. South Am. Earth Sci., 26, 252–260.
- Giambiagi, L., J. Mescua, F. Bechis, A. Tassara, and G. D. Hoke (2012), Thrust belts of the southern Central Andes: Along-strike variations in shortening, topography, crustal geometry, and denudation, *Geol. Soc. Am. Bull.*, 124(7–8), 1339–1351.
- Giambiagi, L. B., P. P. Alvarez, E. Godoy, and V. A. Ramos (2003), The control of pre-existing extensional structures on the evolution of the southern sector of the Aconcagua fold and thrust belt, southern Andes, *Tectonophysics*, 369, 1–19, doi:10.1016/S0040-1951(03)00171-9.
- Godoy, E., G. Yañez, and E. Vera (1999), Inversion of an Oligocene volcano-tectonic basin and uplifting of its superimposed Miocene magmatic arc in the Chilean Central Andes: First seismic and gravity evidences, *Tectonophysics*, *306*, 217–236.
- Grosse, P., F. Söllner, M. A. Báez, A. I. Toselli, J. N. Rossi, and J. D. de la Rosa (2009), Lower Carboniferous post-orogenic granites in central eastern Sierra de Velasco, Sierras Pampeanas, Argentina: U-Pb monazite geochronology, geochemistry and Sr-Nd isotopes, *Int. J. Earth Sci.*, 98, 1001–1025.
- Hilley, G. E., and I. Coutand (2010), Links between topography, erosion, rheological heterogeneity, and deformation in contractional settings: Insights from the central Andes, *Tectonophysics*, 495, 78–92.
- Hoke, G. D., and C. N. Garzione (2008), Paleosurfaces, paleoelevation, and the mechanisms for the late Miocene topographic development of the Altiplano plateau. *Earth Planet. Sci. Lett.*, 271, 192–201.
- Horton, B. K., and F. Fuentes (2016), Sedimentary record of plate coupling and decoupling during growth of the Andes, *Geology*, 44, 647–650. Ingersoll, R. V., T. F. Bullard, R. L. Ford, J. P. Grimm, J. D. Pickle, and S. W. Sares (1984), The effect of grain size on detrital modes: A test of the Gazzi-Dickinson point-counting method, *SEPM J. Sediment. Res.*, 54(1), 103–116.
- Irigoyen, M. V., K. L. Buchan, and R. L. Brown (2000), Magnetostratigraphy of Neogene Andean foreland-basin strata, lat 33°S, Mendoza Province, Argentina, *Geol. Soc. Am. Bull.*, 112, 803–816.
- Johnson, N. M., T. E. Jordan, P. A. Johnson, and C. W. Naeser (1986), Magnetic polarity stratigraphy, age and tectonic setting of fluvial sediments in an eastern Andean foreland basin, San Juan Province, Argentina, Spec. Publ. Int. Assoc. Sedimentol., 8, 63–75.
- Jones, R. E., L. A. Kirstein, S. A. Kasemann, V. D. Litvak, S. Poma, R. N. Alonso, and R. Hinton (2016), The role of changing geodynamics in the progressive contamination of Late Cretaceous to Late Miocene arc magmas in the southern Central Andes, *Lithos*, 262, 169–191.
- Jordan, T. E., P. M. Rutty, L. E. McRae, J. A. Beer, K. Tabbut, and J. F. Damanti (1990), Magnetic polarity stratigraphy of the Miocene Rio Azul section, Precordillera thrust belt, San Juan province, Argentina, J. Geol., 98, 519–539.

- Jordan, T. E., R. W. Allmendinger, J. F. Damanti, and R. E. Drake (1993), Chronology of motion in a complete thrust belt: The Precordillera, 30-31°S, Andes Mountains, *J. Geol.*, 101, 135–156.
- Jordan, T. E., F. Schlunegger, and N. Cardozo (2001), Unsteady and spatially variable evolution of the Neogene Andean Bermejo foreland basin, Argentina, J. South Am. Earth Sci., 14, 775–798.
- Karnauskas, K. B., and C. C. Ummenhofer (2014), On the dynamics of the Hadley circulation and subtropical drying, *Clim. Dyn.*, 42, 2259–2269. Kay, S. M., C. Mpodozis, V. A. Ramos, and F. Munizaga (1991), Magma source variations for mid-late tertiary magmatic rocks associated with a shallowing subduction zone and a thickening crust in the central Andes (28 to 33°S). *Geol. Soc. Am. Spec. Pap.*, 265, 113–138.
- Kley, J., C. R. Monaldi, and J. A. Salfity (1999), Along-strike segmentation of the Andean foreland: Causes and consequences, *Tectonophysics*, 301. 75–94.
- Krapovickas, V., P. L. Ciccioli, M. G. Mángano, C. A. Marsicano, and C. O. Limarino (2009), Paleobiology and paleoecology of an arid-semiarid Miocene South American ichnofauna in anastomosed fluvial deposits, *Palaeogeogr. Palaeoclimatol. Palaeoecol.*, 284, 129–152.
- Levina, M., B. K. Horton, F. Fuentes, and D. F. Stockli (2014), Cenozoic sedimentation and exhumation of the foreland basin system preserved in the Precordillera thrust belt (31–32°S), southern central Andes, Argentina, *Tectonics*, 33, 1659–1680, doi:10.1002/2013TC003424.
- Limarino, C., L. Net, P. Gutierrez, V. Barreda, A. Caselli, and S. Ballent (2000), Definicion litoestratigrafica de la Formacion Cienaga del Rio Huaco (Cretacico Superior), Precordillera central, San Juan, Argentina, Rev. de la Asoc. Geológica Argentina, 55, 83–99.
- Limarino, C., A. Tripaldi, S. Marenssi, L. Net, G. Re, and A. Caselli (2001), Tectonic control on the evolution of the fluvial systems of the Vinchina Formation (Miocene), northwestern Argentina, J. South Am. Earth Sci., 14, 751–762.
- Limarino, C. O., H. L. Sessarego, O. R. López Gamuni, P. R. Gutierrez, and S. N. Césari (1987), Las formaciones Ojo de Agua y Vallecito en el area de la Cienaga, oeste de Huaco, provincia de San Juan: Estratigrafia y paleoambientes sedimentarios, Rev. de la Asoc. Geol. Argentina, 42, 153–167.
- Limarino, C. O., L. A. Fauqué, R. Cardó, M. L. Gagliardo, and L. Escoteguy (2002), La faja volcánica Miocena de la Precordillera septentrional, *Rev. de la Asoc. Geol. Argentina*, *57*, 48–51.
- Litvak, V. D., S. Poma, S. M. Kay, and E. Valle (2007), Paleogene and Neogene magmatism in the Valle del Cura region: New perspective on the evolution of the Pampean flat slab, San Juan province, Argentina, J. South Am. Earth Sci., 24, 117–137.
- Miall, A. D. (1978), Lithofacies types and vertical profile models in braided river deposits: A summary, edited by A. D. Miall, Mem. Can. Soc. Pet. Geol., 5, 597–600.
- Milana, J. P. (1993), Estratigrafía de eolianitas en la zona de Jáchal-Huaco, Precordillera de San Juan, Rev. de la Asoc. Geológica Argentina, 48, 283–298.
- Milana, J. P., F. Bercowski, and T. E. Jordan (2003), Paleoambientes y magnetoestratigrafía del Neógeno de la Sierra de Mogna, y su relación con la Cuenca de Antepaís Andina, *Rev. de la Asoc. Geológica Argentina*, *58*, 447–473.
- Mpodozis, C., and S. M. Kay (1992), Late Paleozoic to Triassic evolution of the Gondwana margin: Evidence from Chilean Frontal cordilleran batholiths (28°S to 31°S), Geol. Soc. Am. Bull., 104, 999–1014.
- Mpodozis, C., and V. A. Ramos (1990), The Andes of Chile and Argentina, in *Geology of the Andes and Its Relation to Hydrocarbon and Mineral Resources, Circumpacific Council for Energy and Mineral Resources*, edited by G. E. Ericksen, M. T. Cañas Pinochet, and J. A. Reinemud, pp. 59–90, Circum-Pacific Council for Energy and Miner. Res., Houston, Tex.
- Oncken, O., G. Chong, G. Franz, P. Giese, H.-J. Gotze, V. A. Ramos, M. R. Strecker, and P. Wigger (2006), *The Andes: Active Subduction Orogeny*, edited by O. Oncken et al., Springer, Berlin.
- Pearson, D. M., P. Kapp, P. W. Reiners, G. E. Gehrels, M. N. Ducea, A. Pullen, J. E. Otamendi, and R. N. Alonso (2012), Major Miocene exhumation by fault-propagation folding within a metamorphosed, early Paleozoic thrust belt: Northwestern Argentina, *Tectonics*, *31*, TC4023, doi:10.1029/2011TC003043.
- Peréz, M. A., F. Fernández Seveso, L. A. Alvarez, and I. E. Brisson (1993), Analisis ambiental y estratigrifico del Paleozoico superior en el area anticlinal de Huaco, San Juan, Argentina, Congrés Int. la Stratigr. geólogie du Carbonifére Permien, Comptes Rendus, 2, 297–318.
- Pingel, H., A. Mulch, R. N. Alonso, J. Cottle, S. A. Hynek, J. Poletti, A. Rohrmann, A. K. Schmitt, D. F. Stockli, and M. R. Strecker (2016), Surface uplift and convective rainfall along the southern Central Andes (Angastaco Basin, NW Argentina), *Earth Planet. Sci. Lett.*, 440, 33–42.
- Quade, J., M. P. Dettinger, B. Carrapa, P. G. DeDelles, K. E. Murray, K. W. Huntington, A. Cartwright, R. R. Canavan, G. Gehrels, and M. Clementz (2015), The growth of the central Andes, 22°S-26°S, *Geol. Soc. Am. Mem.*, 1212, 277–308.
- Ramos, V. A. (2004), Cuyania, an exotic block to Gondwana: Review of a historical success and the present problems, *Gondwana Res.*, 7, 1–18. Ramos, V. A. (2009), Anatomy and global context of the Andes: Main geologic features and the Andean orogenic cycle, *Geol. Soc. Am. Mem.*, 204, 31–65.
- Ramos, V. A., and A. Aleman (2000), Tectonic evolution of the Andes, in *Tectonic evolution of South America*, edited by U. G. Cordani et al., pp. 636–685, Internat. Geol. Congress, Rio de Janeiro.
- Ramos, V. A., M. Cegarra, and E. O. Cristallini (1996), Cenozoic tectonics of the High Andes of west-central Argentina (30–36°S latitude), *Tectonophysics*, 259, 185–200.
- Ramos, V. A., E. O. Cristallini, and D. J. Pérez (2002), The Pampean flat-slab of the Central Andes, J. South Am. Earth Sci., 15, 59–78.
- Reat, E. J. (2016), Paleogeography and Depositional Systems of Cretaceous-Oligocene Strata: Eastern Precordillera, Indiana Univ., Argentina.
- Rossel, K., G. Aguilar, E. Salazar, J. Martinod, S. Carretier, L. Pinto, and A. Cabré (2016), Chronology of Chilean Frontal Cordillera building from geochronological, stratigraphic and geomorphological data insights from Miocene intramontane-basin deposits, *Basin Res.*, 1–22, doi:10.1111/bre.12221.
- Ruskin, B. G., F. M. Dávila, G. D. Hoke, T. E. Jordan, R. A. Astini, and R. Alonso (2011), Stable isotope composition of middle Miocene carbonates of the Frontal Cordillera and Sierras Pampeanas: Did the Paranaense seaway flood western and central Argentina?, *Palaeogeogr. Palaeoecol.*, 308, 293–303.
- Safipour, R., B. Carrapa, P. G. DeCelles, and S. N. Thomson (2015), Exhumation of the Precordillera and northern Sierras Pampeanas and along-strike correlation of the Andean orogenic front, northwestern Argentina, *Geol. Soc. Am. Mem.*, 212, 181–199.
- SERNAGEOMIN (2003), Mapa Geológico de Chile: versión digital. Servicio Nacional de Geología y Minería, Publicación Geológica Digital, No. 4 (CD-ROM, version 1.0, 2003), Santiago.
- Soria, T. B. (2010), Geología de la Formación Ciénaga del Río Huaco (Cretacico), al norte del Río Huaco, Departamento Jáchal, Provincia de San Juan, Argentina, Final work of Licenciatura en Geología, Universidad Nacional de San Juan.
- Strecker, M. R., R. N. Alonso, B. Bookhagen, B. Carrapa, G. E. Hilley, E. Sobel, and M. H. Trauth (2007), Tectonics and climate of the Southern Central Andes, *Annu. Rev. Earth Planet. Sci.*, 35, 747–787.
- Suriano, J., M. S. Alonso, C. O. Limarino, and A. M. Tedesco (2011), La Formación Cuesta del Viento: Una nueva unidad litoestratigráfica en la evolución del orógeno Precordillerano, *Rev. de la Asoc. Geol. Argentina*, 68, 246–260.
- Tankard, A. J., et al. (1995), Structural and tectonic controls of basin evolution in southwestern Gondwana during the Phanerozoic, AAPG Mem., 62, 5–52.

Tectonophysics, 583, 105-123.

- Tedesco, A. M., and C. O. Limarino (2007), Primera edad radimétrica de los depósitos Cretácicos de la Precordillera Central, Rev. de la Asoc. Geol. Argentina, 62, 471–474.
- Tello, R. (2013), Áreas Protegidas de la Provincia de San Juan, Secretaría de Ambiente y Desarrollo Sustentable, Gobierno de la Provincia de San Juan, San Juan, Argentina.
- Thomas, W. A., and R. A. Astini (1996), The Argentine Precordillera: A traveler from the Ouachita Embayment of North American Laurentia, *Science. 273*, 752–757.
- Tripaldi, A., and C. O. Limarino (2005), Vallecito Formation (Miocene): The evolution of an eolian system in an Andean foreland basin (northwestern Argentina), *J. South Am. Earth Sci.*, 19, 343–357.
- Val, P., G. D. Hoke, J. C. Fosdick, and H. Wittmann (2016), Reconciling tectonic shortening, sedimentation and spatial patterns of erosion from <sup>10</sup>Be paleo-erosion rates in the Argentine Precordillera, *Earth Planet. Sci. Lett.*, 450, 173–18.
- van Hinsbergen, D. J. J., L. V. de Groot, S. J. van Schaik, W. Spakman, P. K. Bijl, A. Sluijs, C. G. Langereis, and H. Brinkhuis (2015), A paleolatitude calculator for paleoclimate studies, *PLoS One*, *10*, e0126946, doi:10.1371/journal.pone.0126946.
- van Hinte, J. E. (1978), Geohistory analysis application of micropaleontology in exploration geology, *Am. Assoc. Pet. Geol. Bull.*, *62*, 201–222. Vizán, H., S. Geuna, R. Melchor, E. S. Bellosi, S. L. Lagorio, C. Vásquez, M. S. Japas, G. Ré, and M. Do Campo (2013), Geological setting and paleomagnetism of the Eocene red beds of Laguna Brava Formation (Quebrada Santo Domingo, northwestern Argentina),
- Walcek, A. A., and G. D. Hoke (2012), Surface uplift and erosion of the southernmost Argentine Precordillera, *Geomorphology*, 153–154, 156–168.
- Willett, S. D. (1999), Orogeny and orography: The effects of erosion on the structure of mountain belts, *J. Geophys. Res.*, 104, 28,957–28,981, doi:10.1029/1999JB900248.
- Winocur, D. A., V. D. Litvak, and V. A. Ramos (2014), Magmatic and tectonic evolution of the Oligocene Valle del Cura basin, main Andes of Argentina and Chile: Evidence for generalized extension, in *Geodynamic Processes Andes Central Chile Argentina, Geol. Soc. London, Spec. Publ.*, vol. 399, edited by P. Sepulveda et al., pp. 109–130.
- Yrigoyen, M. (1993), Los depósitos sinorogénicos Terciarios, in *Geología y Recursos Naturales de Mendoza*, edited by V. Ramos, pp. 123–148, Congreso Geológico Argentino y II Congreso de Exploración de Hidrocarburos, Relatorio, Mendoza, Argentina.
- Zachos, J. C., G. R. Dickens, and R. E. Zeebe (2008), An early Cenozoic perspective on greenhouse warming and carbon-cycle dynamics, *Nature*, 451, 279–283.
- Zapata, T. R. (1998), Crustal structure of the Andean thrust front at 30°S latitude from shallow and deep seismic reflection profiles, Argentina, J. South Am. Earth Sci., 11, 131–151.
- Zapata, T. R., and R. W. Allmendinger (1996), Growth stratal records of instantaneous and progressive limb rotation in the Precordillera thrust belt and Bermejo basin, Argentina, *Tectonics*, 15, 1065–1083, doi:10.1029/96TC00431.